

Modeling High-Dimensional Matrix-Variate Observations by Tensor Factorization

Xu Zhang

School of Mathematical Science, South China Normal University, China.

Zhen Pang

Department of Applied Mathematics, The Hong Kong Polytechnic University, HKSAR, China.

Jianhua Guo

School of Mathematics and Statistics, Northeast Normal University, China.

Alan H. Welsh

Research School of Finance, Actuarial Studies and Statistics, The Australian National University, Australia.

Catherine C. Liu

Department of Applied Mathematics, The Hong Kong Polytechnic University, Hong Kong SAR.

†E-mail: macliu@polyu.edu.hk

Summary. In the era of big data, it is prevailing of high-dimensional matrix-variate observations that may be independent or dependent. Unsupervised learning of matrix objects through low-rank approximation has benefited discovery of the hidden pattern and structure whilst concomitant statistical inference is known challenging and yet in infancy by the fact that, there is limited work and all focus on a class of bilinear form matrix factor models. In this paper, we propose a novel class of hierarchical CP product matrix factor

†*Address for correspondence:* Catherine C. Liu, Department of Applied Mathematics, The Hong Kong Polytechnic University, Hung Hom, Kowloon, HKSAR, China

models which model the rank-1 components of the low-rank CP decomposition of a matrix object by the tool of high-dimensional vector factor models. The induced CP tensor-decomposition based matrix factor model (TeDFaM) are apparently more informative in that it naturally incorporates the row-wise and column-wise interrelated information. Furthermore, the inner separable covariance structure yields efficient moment estimators of the loading matrices and thus approximate least squares estimators for the factor scores. The proposed TeDFaM model and estimation procedure make the signal part achieves better peak signal to noise ratio, evidenced in both theory and numerical analytics compared to bilinear form matrix factor models and existing methods. We establish an inferential theory for TeDFaM estimation including consistency, rates of convergence, and the limiting distributions under regular conditions. In applications, the proposed model and estimation procedure are superior in terms of matrix reconstruction for both independent two-dimensional image data and serial correlated matrix time series. The algorithm is fast and can be implemented expediently through an accompanied R package TeDFaM.

Keywords: Moment Estimation; Matrix Factor Model; Image Reconstruction; Separable Covariance Structure; Signal-to-Noise Ratio; Tensor CP Decomposition; Tensor Subspace

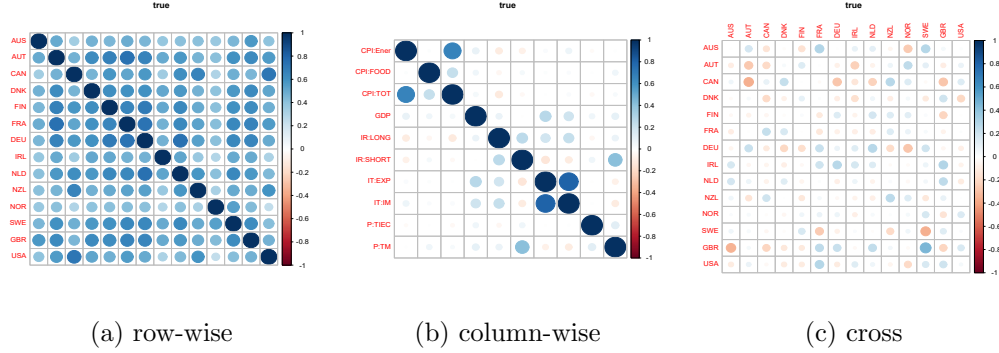
1. Introduction

With the contemporary data acquisition techniques, high-dimensional matrix-variate observations are booming in finance, economics, sociology, epidemiology, and machine learning (Zhang, 2017; Gupta and Nagar, 2018; Fan et al., 2020). Unsupervised learning for collections of matrix-variate observations focuses on finding the hidden pattern and latent structure that can separate the signal from the noise. Inspired by the fact that factor models are natural workhorses that resolve dimension reduction and latent feature extraction, we propose a novel matrix factor model, to be called TeDFaM in this article, and establish its inferential theory so that one may deal with collections of matrix-variate observations for multiple purposes of matrix reconstruction, supervised learning, and or so.

There is wealth of literature in researching high-dimensional *vector* factor models (Bai (2003); Lam and Yao (2011, 2012); Bai and Li (2012), among others), while there

is sporadic work studying in inferential theory of high-dimensional *matrix* factor models (Wang et al., 2019; Chen and Fan, 2021; Yu et al., 2022). To the best of our knowledge, available publication all focus on the *bilinear form* matrix factor model (BiMFaM), where the signal part is the product of the low-dimensional latent factor with the left-side multiplier of the row loading matrix and the right-side multiplier of the column loading matrix. That is, bilinear form approximation has good interpretation in the role of the signal part of a matrix object, in that the rows and columns of the smaller matrix of the bilinear form represent linear combinations of row and column elements of the raw high-dimensional matrix respectively (Ye (2005); Li et al. (2010); Ding and Dennis Cook (2018); Chen et al. (2020a), among others). Note that existing estimation approaches within BiMFaM are all data driven since data characteristics such as time series or uncorrelated will be their first concern in developing the methodology.

The rationale of BiMFaM is that such bilinear form signal preserves the original matrix structure in a low-rank matrix approximation, and thus maintains the interpretation of rows and columns, say, one may locate particular rows or columns as if their interaction took impact on the signal. Nevertheless, pure row-wise or pure column-wise information may exist and strengthen the signal, and should NOT be omitted. For instance, let us look into the common multinational macroeconomic indices data, which are collected quarterly over a certain time period in years for multiple countries from OECD, and can be integrally treated as matrix-variate observations with rows and columns representing different countries and macroeconomic indices respectively, and each element representing the value of the index of the corresponding country. Figure 1 (a), (b), and (c) show correlation heatmaps of the row-wise (country), the column-wise (index), and interacted between rows and columns, respectively. Because of the geographical, historical, economic and political relationship of countries, there exists positive correlation among countries (rows) and obvious correlation among indices (columns) such as the CPI group and international trade group. Figure 1 (c) plots the correlation cross the first and the third indices (columns) among different countries (rows), where the non-diagonal elements show that there exist sign varying correlation cross different rows and columns. Consequently, neglecting the pure row or the pure column interrelated infor-

**Fig. 1.** True correlation of data

mation may impair inferential results of unsupervised learning, which will be illustrated in our numerical analysis later.

These shed light on our spirit of modeling, that we attempt to formulate a new efficient matrix factor model, which will not neglect any mode-wise structural information, and can always work robustly regardless of independence or dependence of the sequence of matrix-variate observations. Our proposed CP tensor-decomposition based matrix factor model (TeDFaM) has the low rank approximation in the sum of THREE terms, making the inferential procedure challenging. For example, one can not estimate the loading matrix parameters and factor scores simultaneously based on traditional spectral decomposition. Though incorporating the extra row-wise and column-wise terms will slow down the theoretical convergence rate of the estimated loading matrices, the reconstruction performance behaves better than solely the bilinear form signal without extra computation burden. In addition, from the perspective of distribution, the proposed model can be regarded as the explicit model form of the matrix-variate distribution with the separable covariance structure (Dawid, 1981; Hoff, 2011; Gupta and Nagar, 2018). This observation alleviates the challenge in estimation of the complicated new matrix factor model.

The remainder of this article is organized as follows. Section 2 proposes the tensor-decomposition based matrix factor model, the approximate estimation algorithm, and the theoretical comparison of reconstruction error between the TeDFaM and the BiM-FaM. Section 3 establishes the theoretical properties of the estimated loading matrices

and the signal part. Section 4 contains the simulation studies to evaluate the finite sample performance. Section 5 analyzes the multinational macroeconomic indices data, and the CT image data collected during early COVID-19 pandemic. Section 6 concludes the paper with some further research topics. All the technical proofs are left in the supplementary materials.

2. Tensor-decomposition based matrix factor model

2.1. Modelling

Let $\mathbf{X}_t \in \mathbb{R}^{p_1 \times p_2}$, $1 \leq t \leq T$, be the observed rank- l high-dimensional matrix-variate that may be uncorrelated or serial correlated, where T , p_1 , and p_2 can be sufficiently large. We postulate the following hierarchical *CP product matrix factor model*, which integrates the low-rank CP decomposition (Kolda and Bader, 2009, Section 3) of a matrix variable with low-rank vector factor models of its inner rank-one-components,

$$\begin{cases} \mathbf{X}_t = \sum_{i=1}^l \mathbf{U}_{t,i} \circ \mathbf{V}_{t,i}, \\ \mathbf{U}_{t,i} = \mathbf{R}\mathbf{A}_{t,i} + \boldsymbol{\xi}_{t,i}, \\ \mathbf{V}_{t,i} = \mathbf{C}\mathbf{B}_{t,i} + \boldsymbol{\eta}_{t,i}. \end{cases} \quad (1)$$

Here $\mathbf{U}_{t,i} \in \mathbb{R}^{p_1}$ and $\mathbf{V}_{t,i} \in \mathbb{R}^{p_2}$ are rank-one components of the low-rank CP factorization of \mathbf{X}_t ; for the inner high-dimensional vectors $\mathbf{U}_{t,i}$ and $\mathbf{V}_{t,i}$, we nest the low-rank representation by the tool of vector factor model (Bai, 2003, Equation (3)), where $\mathbf{R} \in \mathbb{R}^{p_1 \times k_1}$ and $\mathbf{C} \in \mathbb{R}^{p_2 \times k_2}$ ($k_1 \ll p_1$ and $k_2 \ll p_2$) are factor loading matrices, $\mathbf{A}_{t,i} \in \mathbb{R}^{k_1}$ and $\mathbf{B}_{t,i} \in \mathbb{R}^{k_2}$ are low-dimensional latent factors, $\boldsymbol{\xi}_{t,i} \in \mathbb{R}^{p_1}$ and $\boldsymbol{\eta}_{t,i} \in \mathbb{R}^{p_2}$ are idiosyncratic errors, and \circ is the outer product operation.

Using the matrix notation, we have factor matrices of \mathbf{X}_t under the CP decomposition as $\mathbf{U}_t = (\mathbf{U}_{t,1}, \dots, \mathbf{U}_{t,l}) \in \mathbb{R}^{p_1 \times l}$ and $\mathbf{V}_t = (\mathbf{V}_{t,1}, \dots, \mathbf{V}_{t,l}) \in \mathbb{R}^{p_2 \times l}$, the latent factor matrices of \mathbf{U}_t and \mathbf{V}_t under vector factor models as $\mathbf{A}_t = (\mathbf{A}_{t,1}, \dots, \mathbf{A}_{t,l})^\top \in \mathbb{R}^{l \times k_1}$ and $\mathbf{B}_t = (\mathbf{B}_{t,1}, \dots, \mathbf{B}_{t,l})^\top \in \mathbb{R}^{l \times k_2}$, and error matrices of \mathbf{U}_t and \mathbf{V}_t as $\boldsymbol{\xi}_t = (\boldsymbol{\xi}_{t,1}, \dots, \boldsymbol{\xi}_{t,l}) \in \mathbb{R}^{p_1 \times l}$ and $\boldsymbol{\eta}_t = (\boldsymbol{\eta}_{t,1}, \dots, \boldsymbol{\eta}_{t,l}) \in \mathbb{R}^{p_2 \times l}$. Assume $\{\mathbf{A}_t\}_{t=1}^T$, $\{\mathbf{B}_t\}_{t=1}^T$, $\{\boldsymbol{\xi}_t\}_{t=1}^T$ and $\{\boldsymbol{\eta}_t\}_{t=1}^T$ are zero mean and mutually uncorrelated. Then expanding model (1) yields the following

equivalent representation

$$\mathbf{X}_t = \mathbf{R}\mathbf{A}_t^\top \mathbf{B}_t \mathbf{C}^\top + \mathbf{R}\mathbf{A}_t^\top \boldsymbol{\eta}_t^\top + \boldsymbol{\xi}_t \mathbf{B}_t \mathbf{C}^\top + \boldsymbol{\xi}_t \boldsymbol{\eta}_t^\top.$$

Let $\mathbf{Z}_t = \mathbf{A}_t^\top \mathbf{B}_t$, $\mathbf{E}_t = \boldsymbol{\eta}_t \mathbf{A}_t$, $\mathbf{F}_t = \boldsymbol{\xi}_t \mathbf{B}_t$, and $\mathbf{e}_t = \boldsymbol{\xi}_t \boldsymbol{\eta}_t^\top$. Then series $\{\mathbf{Z}_t\}_{t=1}^T$, $\{\mathbf{E}_t\}_{t=1}^T$, $\{\mathbf{F}_t\}_{t=1}^T$, and $\{\mathbf{e}_t\}_{t=1}^T$ are zero mean and mutually uncorrelated. Hence model (1) is transformed to the following *tensor-decomposition based matrix factor model* (TeDFaM)

$$\begin{aligned} \mathbf{X}_t &= \mathbf{S}_t + \mathbf{e}_t, \\ \mathbf{S}_t &= \mathbf{R}\mathbf{Z}_t \mathbf{C}^\top + \mathbf{R}\mathbf{E}_t^\top + \mathbf{F}_t \mathbf{C}^\top, \end{aligned} \quad (2)$$

where $\mathbf{S}_t \in \mathbb{R}^{p_1 \times p_2}$ and $\mathbf{e}_t \in \mathbb{R}^{p_1 \times p_2}$ represent the unknown signal and noise parts of \mathbf{X}_t . In the signal part, $\mathbf{Z}_t \in \mathbb{R}^{k_1 \times k_2}$ is the low-dimensional global latent matrix factors, and $\mathbf{E}_t \in \mathbb{R}^{p_2 \times k_1}$ and $\mathbf{F}_t \in \mathbb{R}^{p_1 \times k_2}$ are mode-wise latent factors of the column and the row, respectively. It is known that estimates of \mathbf{R} and \mathbf{C} are not unique unless allowing some kind of rotation (Wang et al., 2019; Chen and Fan, 2021); in our case, we assume that $p_1^{-1} \mathbf{R}^\top \mathbf{R} \approx \mathbf{I}_{k_1}$ and $p_2^{-1} \mathbf{C}^\top \mathbf{C} \approx \mathbf{I}_{k_2}$, which are called the strong factor assumption in literature of factor models (Stock and Watson, 2002; Lam and Yao, 2011). In Assumption 3 of Section 4, we will provide the strict limit forms of the strong factor assumption.

2.2. Covariance Decomposition

For the proposed new matrix factor model (2), we may see its strong intuitive interpretation from the insight of the contribution of the three latent factors to the covariance of any pair of entries of the t th observation. Without loss of generality, assume that \mathbf{E}_t and \mathbf{F}_t are row independent, and \mathbf{e}_t is i.i.d.. Then by some algebra, the covariance of two entries $\mathbf{X}_{t,i_1 j_1}$ and $\mathbf{X}_{t,i_2 j_2}$ is

$$\begin{aligned} \text{cov}(\mathbf{X}_{t,i_1 j_1}, \mathbf{X}_{t,i_2 j_2}) &= \mathbf{R}_{i_1}^\top \mathbb{E}(\mathbf{Z}_t \mathbf{C}_{j_1} \mathbf{C}_{j_2}^\top \mathbf{Z}_t^\top) \mathbf{R}_{i_2} + \mathbf{R}_{i_1}^\top \mathbb{E}(\mathbf{E}_{t,j_1} \mathbf{E}_{t,j_2}^\top) \mathbf{R}_{i_2} \\ &\quad + \mathbf{C}_{j_1}^\top \mathbb{E}(\mathbf{F}_{t,i_1} \mathbf{F}_{t,i_2}^\top) \mathbf{C}_{j_2} + \mathbb{E}(\mathbf{e}_{t,i_1 j_1} \mathbf{e}_{t,i_2 j_2}). \end{aligned}$$

We can see that the summand of the covariance expansion that contains \mathbf{F}_t is nonzero only for two entries in the same row (i.e., $i_1 = i_2$), which means that \mathbf{F}_t reflects the pure row-wise correlation of the matrix observation. Similarly, the summand of the covariance expansion that contains \mathbf{E}_t is nonzero only for two entries in the same column (i.e.,

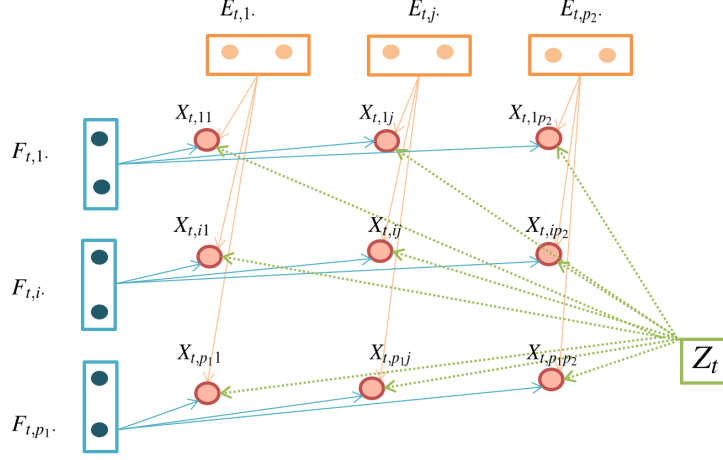


Fig. 2. Bayesian network for the TeDFaM

$j_1 = j_2$), which means that \mathbf{E}_t reflects the pure column-wise correlation of the matrix observation. Nevertheless the summand of the covariance that contains \mathbf{Z}_t always being nonzero for any pair of indices, which means that \mathbf{Z}_t combines the row-wise, column-wise, and the across modes correlation of the matrix observation. In this sense, the bilinear form $\mathbf{R}\mathbf{Z}_t\mathbf{C}^\top$ characterizes the interaction effects, and the two linear forms $\mathbf{R}\mathbf{E}_t^\top$ and $\mathbf{F}_t\mathbf{C}^\top$ characterize the pure column and the pure row effects, respectively. We use the the Bayesian network in Figure 2 to demonstrate the relationship of three latent factors and the matrix observation, where \mathbf{Z}_t , \mathbf{F}_t and \mathbf{E}_t influence every entry, the rows and the columns of the matrix observation \mathbf{X}_t , respectively.

2.3. Tensor Subspace Learning

We look into the signal \mathbf{S}_t of the TeDFaM from the perspective of tensor subspace learning (Lu et al., 2013). For our proposed low-rank approximation \mathbf{S}_t of the matrix variate, the corresponding low-dimensional tensor subspace \mathcal{S}_{non} is written as

$$\mathcal{S}_{non} = \left\{ \sum_{i_1=1}^{k_1} \sum_{i_2=1}^{k_2} Z_{i_1 i_2} (\mathbf{R}_{\cdot i_1} \circ \mathbf{C}_{\cdot i_2}) + \sum_{i_1=1}^{k_1} \sum_{i_2=1}^{p_2} E_{i_2 i_1} (\mathbf{R}_{\cdot i_1} \circ \mathbf{I}_{p_2, \cdot i_2}) + \sum_{i_1=1}^{p_1} \sum_{i_2=1}^{k_2} F_{i_1 i_2} (\mathbf{I}_{p_1, \cdot i_1} \circ \mathbf{C}_{\cdot i_2}) \right. \\ \left. | \mathbf{Z} = (Z_{i_1 i_2}) \in \mathbb{R}^{k_1 \times k_2}, \mathbf{E} = (E_{i_2 i_1}) \in \mathbb{R}^{p_2 \times k_1}, \mathbf{F} = (F_{i_1 i_2}) \in \mathbb{R}^{p_1 \times k_2} \right\},$$

where $\mathbf{R}_{\cdot i_1}$ and $\mathbf{C}_{\cdot i_2}$ are the i_1 th and the i_2 th columns of \mathbf{R} and \mathbf{C} , and \mathbf{I}_{p_1, i_1} and \mathbf{I}_{p_2, i_2} are the i_1 th and the i_2 th columns of the p_1 -dim and p_2 -dim identity matrices.

To demonstrate the dimension of \mathcal{S}_{non} , we first introduce the definition of the tensor product (Merris, 1997). A tensor product of two vector spaces V and W is a vector space denoted as $V \otimes W$ (pronounced V tensor W), where \otimes is a bilinear map $\otimes : V \times W \rightarrow V \otimes W$, $(v, w) \mapsto v \otimes w$ satisfying the universal property, i.e., for any bilinear map $b : V \times W \rightarrow U$ there is a unique linear map $\bar{b} : V \otimes W \rightarrow U$ such that $\bar{b}(v \otimes w) = b(v, w)$. In addition, If $\{v_i\}$ and $\{w_j\}$ are bases of V and W respectively, then $\{v_i \otimes w_j\}$ is a basis of $V \otimes W$.

By taking the bilinear map \otimes as the Kronecker product operation and taking vectorization operation $\text{vec}(\cdot)$ on $\mathbf{R}_{\cdot i_1} \circ \mathbf{C}_{\cdot i_2}$, $\mathbf{R}_{\cdot i_1} \circ \mathbf{I}_{p_2, i_2}$, and $\mathbf{I}_{p_1, i_1} \circ \mathbf{C}_{\cdot i_2}$ result in $\text{vec}(\mathbf{R}_{\cdot i_1} \circ \mathbf{C}_{\cdot i_2}) = \mathbf{C}_{\cdot i_2} \otimes \mathbf{R}_{\cdot i_1}$, $\text{vec}(\mathbf{R}_{\cdot i_1} \circ \mathbf{I}_{p_2, i_2}) = \mathbf{I}_{p_2, i_2} \otimes \mathbf{R}_{\cdot i_1}$, and $\text{vec}(\mathbf{I}_{p_1, i_1} \circ \mathbf{C}_{\cdot i_2}) = \mathbf{C}_{\cdot i_2} \otimes \mathbf{I}_{p_1, i_1}$, respectively. Then $\{\mathbf{C}_{\cdot i_2} \otimes \mathbf{R}_{\cdot i_1} : i_1 \in [k_1], i_2 \in [k_2]\}$ is the basis of the tensor product $\text{span}(\mathbf{C}) \otimes \text{span}(\mathbf{R})$, $\{\mathbf{I}_{p_2, i_2} \otimes \mathbf{R}_{\cdot i_1} : i_1 \in [k_1], i_2 \in [p_2]\}$ is the basis of the tensor product $\mathbb{R}^{p_2} \otimes \text{span}(\mathbf{R})$, and $\{\mathbf{C}_{\cdot i_2} \otimes \mathbf{I}_{p_1, i_1} : i_1 \in [p_1], i_2 \in [k_2]\}$ is the basis of the tensor product $\text{span}(\mathbf{C}) \otimes \mathbb{R}^{p_1}$, where $\text{span}(\mathbf{R})$ and $\text{span}(\mathbf{C})$ are the spaces spanned by the columns of \mathbf{R} and \mathbf{C} , and $[n] = \{1, \dots, n\}$ with n as the placeholder. We can see that $\text{span}(\mathbf{C}) \otimes \text{span}(\mathbf{R})$ is contained in $\mathbb{R}^{p_2} \otimes \text{span}(\mathbf{R})$ or $\text{span}(\mathbf{C}) \otimes \mathbb{R}^{p_1}$. As a result, the tensor subspace \mathcal{S}_{non} turns to the following vectorization subspace

$$\tilde{\mathcal{S}}_{non} = \left\{ \sum_{i_1=1}^{k_1} \sum_{i_2=1}^{k_2} Z_{i_1 i_2} (\mathbf{C}_{\cdot i_2} \otimes \mathbf{R}_{\cdot i_1}) + \sum_{i_1=1}^{k_1} \sum_{i_2=1}^{p_2} E_{i_2 i_1} (\mathbf{I}_{p_2, i_2} \otimes \mathbf{R}_{\cdot i_1}) + \sum_{i_1=1}^{p_1} \sum_{i_2=1}^{k_2} F_{i_1 i_2} (\mathbf{C}_{\cdot i_2} \otimes \mathbf{I}_{p_1, i_1}) \right. \\ \left. | \mathbf{Z} = (Z_{i_1 i_2}) \in \mathbb{R}^{k_1 \times k_2}, \mathbf{E} = (E_{i_2 i_1}) \in \mathbb{R}^{p_2 \times k_1}, \mathbf{F} = (F_{i_1 i_2}) \in \mathbb{R}^{p_1 \times k_2} \right\}.$$

Therefore, the dimension of $\tilde{\mathcal{S}}_{non}$ or \mathcal{S}_{non} is

$$\dim(\mathcal{S}_{non}) = \dim(\tilde{\mathcal{S}}_{non}) = p_1 k_2 + k_1 p_2 - \dim\{\text{span}(\mathbf{I}_{p_2} \otimes \mathbf{R}) \cap \text{span}(\mathbf{C} \otimes \mathbf{I}_{p_1})\} \ll p_1 p_2.$$

Remark 1. *Bilinear matrix factor model.* A commonly studied bilinear matrix factor model (Wang et al., 2019; Chen and Fan, 2021; Yu et al., 2022), which is called BiMFaM in our paper thereafter, has the following form as

$$\mathbf{X}_t = \mathbf{R} \mathbf{Z}_t \mathbf{C}^\top + \mathbf{e}_t, \quad (3)$$

where only the bilinear form $\mathbf{R} \mathbf{Z}_t \mathbf{C}^\top$ represents the signal. From a tensor insight, the signal part can be rewritten as $\mathbf{Z}_t \times_1 \mathbf{R} \times_2 \mathbf{C}$, which is precisely the 2nd-order case of the

well-known Tucker tensor decomposition (Kolda and Bader, 2009). The low-dimensional tensor subspace \mathcal{S}_{bi} and the vectorization subspace $\tilde{\mathcal{S}}_{bi}$ of the BiMFaM are

$$\mathcal{S}_{bi} = \left\{ \sum_{i_1=1}^{k_1} \sum_{i_2=1}^{k_2} Z_{i_1 i_2} (\mathbf{R}_{\cdot i_1} \circ \mathbf{C}_{\cdot i_2}) \mid \mathbf{Z} = (Z_{i_1 i_2}) \in \mathbb{R}^{k_1 \times k_2} \right\},$$

$$\tilde{\mathcal{S}}_{bi} = \left\{ \sum_{i_1=1}^{k_1} \sum_{i_2=1}^{k_2} Z_{i_1 i_2} (\mathbf{C}_{\cdot i_2} \otimes \mathbf{R}_{\cdot i_1}) \mid \mathbf{Z} = (Z_{i_1 i_2}) \in \mathbb{R}^{k_1 \times k_2} \right\},$$

respectively. Apparently, we have $\dim(\mathcal{S}_{bi}) = \dim(\tilde{\mathcal{S}}_{bi}) = k_1 k_2$.

Remark 2. *BiMFaM v.s. TeDFaM.* The dimension of tensor subspace of the BiMFaM is much less than that of the TeDFaM. Hence the BiMFaM has the advantage of better theoretical convergence rate of the low-rank components due to the lower dimension of the tensor subspace \mathcal{S}_{bi} (only the global latent factors \mathbf{Z}_t are involved). Comparatively, the proposed TeDFaM sacrifices the efficiency on the dimension reduction side due to the additional column and row latent factors \mathbf{E}_t and \mathbf{F}_t , which extract more information that is beyond what bilinear form signal can contribute. Consequently, the performance in the the matrix reconstruction side is no doubt better, which is strictly evidenced by our Proposition 1 in the next section. Last but not least, the unknown parameters \mathbf{R} and \mathbf{C} in the TeDFaM are the same to that in the BiMFaM, and hence the proposed model has no extra computation burden.

3. Estimation

We list notations that will be used thereafter. Let $\mathbf{1}_l$ be the l -dim vector with all entries unit, $\text{eig}(\mathbf{U}, r)$ be the matrix with columns being the top r eigenvectors of \mathbf{U} descendingly, \otimes be the Kronecker product, and \odot be the Khatri-Rao product of two matrices $\mathbf{A} \in \mathbb{R}^{I \times K}$ and $\mathbf{B} \in \mathbb{R}^{J \times K}$ defined by $\mathbf{A} \odot \mathbf{B} = (\mathbf{A}_{\cdot 1} \otimes \mathbf{B}_{\cdot 1}, \dots, \mathbf{A}_{\cdot K} \otimes \mathbf{B}_{\cdot K}) \in \mathbb{R}^{(IJ) \times K}$, where generically $\mathbf{U}_{\cdot i}$ is the i th columns of \mathbf{U} .

3.1. Moment Estimation for Factor Loadings

Taking the vectorization operator on the matrix observations based model (2), one has

$$\text{vec}(\mathbf{X}_t) = (\mathbf{C} \otimes \mathbf{R})\text{vec}(\mathbf{Z}_t) + (\mathbf{I}_{p_2} \otimes \mathbf{R})\text{vec}(\mathbf{E}_t^\top) + (\mathbf{C} \otimes \mathbf{I}_{p_1})\text{vec}(\mathbf{F}_t) + \text{vec}(\mathbf{e}_t), \quad (4)$$

where $\text{vec}(\mathbf{Z}_t) = (\mathbf{B}_t^\top \odot \mathbf{A}_t^\top) \mathbf{1}_l$, $\text{vec}(\mathbf{E}_t) = (\mathbf{A}_t^\top \odot \boldsymbol{\eta}_t) \mathbf{1}_l$, $\text{vec}(\mathbf{F}_t) = (\mathbf{B}_t^\top \odot \boldsymbol{\xi}_t) \mathbf{1}_l$, and $\text{vec}(\mathbf{e}_t) = (\boldsymbol{\eta}_t \odot \boldsymbol{\xi}_t) \mathbf{1}_l$.

In the first expression of CP decomposition in model (1), assume that the rank-one components $\mathbf{U}_{t,i}$ are uncorrelated without loss of generality. Hence in their low-rank vector factor model representations, the latent factors $\mathbf{A}_{t,i}$ and the idiosyncratic errors $\boldsymbol{\xi}_{t,i}$ are uncorrelated, respectively; and so are the other rank-one components $\mathbf{V}_{t,i}$, and the accompanied $\mathbf{B}_{t,i}$ and $\boldsymbol{\eta}_{t,i}$. Let $\boldsymbol{\Psi}_A \in \mathbb{R}^{k_1 \times k_1}$ and $\boldsymbol{\Psi}_B \in \mathbb{R}^{k_2 \times k_2}$ be the variance-covariance matrices of $\mathbf{A}_{t,i}$ and $\mathbf{B}_{t,i}$, respectively, and $\boldsymbol{\Psi}_\xi \in \mathbb{R}^{p_1 \times p_1}$ and $\boldsymbol{\Psi}_\eta \in \mathbb{R}^{p_2 \times p_2}$ be the variance-covariance matrices of $\boldsymbol{\xi}_{t,i}$ and $\boldsymbol{\eta}_{t,i}$ respectively.

The uncorrelation of $\mathbf{U}_{t,i}$ and $\mathbf{V}_{t,i}$ guarantees that \mathbf{Z}_t , \mathbf{E}_t , \mathbf{F}_t , and \mathbf{e}_t have the separable covariance structure (Hoff, 2011) under model (2), modeled by $\text{cov}\{\text{vec}(\mathbf{Z}_t)\} = l(\boldsymbol{\Psi}_B \otimes \boldsymbol{\Psi}_A)$, $\text{cov}\{\text{vec}(\mathbf{E}_t)\} = l(\boldsymbol{\Psi}_A \otimes \boldsymbol{\Psi}_\eta)$, $\text{cov}\{\text{vec}(\mathbf{F}_t)\} = l(\boldsymbol{\Psi}_B \otimes \boldsymbol{\Psi}_\xi)$, and $\text{cov}\{\text{vec}(\mathbf{e}_t)\} = l(\boldsymbol{\Psi}_\eta \otimes \boldsymbol{\Psi}_\xi)$. By quick algebra, \mathbf{X}_t has a separable covariance structure under model (4) since

$$\text{cov}\{\text{vec}(\mathbf{X}_t)\} = l(\mathbf{C}\boldsymbol{\Psi}_B\mathbf{C}^\top + \boldsymbol{\Psi}_\eta) \otimes (\mathbf{R}\boldsymbol{\Psi}_A\mathbf{R}^\top + \boldsymbol{\Psi}_\xi) =: l(\boldsymbol{\Sigma}_2 \otimes \boldsymbol{\Sigma}_1). \quad (5)$$

where $\boldsymbol{\Sigma}_1 \in \mathbb{R}^{p_1 \times p_1}$ represents the column-wise variance-covariance matrix of \mathbf{X}_t and controls the correlation among different rows, and $\boldsymbol{\Sigma}_2 \in \mathbb{R}^{p_2 \times p_2}$ represents the row-wise variance-covariance matrix of \mathbf{X}_t and controls the correlation among different columns. It yields $\mathbb{E}(\mathbf{X}_{t,i_1 j_1} \mathbf{X}_{t,i_2 j_2}) = l \boldsymbol{\Sigma}_{1,i_1 i_2} \boldsymbol{\Sigma}_{2,j_1 j_2}$ by the separable covariance structure of \mathbf{X}_t modeled in equation (5). Hence we have the second-order column-wise population moment

$$\mathbb{E}(\mathbf{X}_t \mathbf{X}_t^\top) = \{l \text{tr}(\boldsymbol{\Sigma}_2)\} \boldsymbol{\Sigma}_1,$$

the (i_1, i_2) th entry of which is $\mathbb{E}(\mathbf{X}_{t,i_1}^\top \mathbf{X}_{t,i_2}) = \sum_{j=1}^{p_2} \mathbb{E}(\mathbf{X}_{t,i_1 j} \mathbf{X}_{t,i_2 j}) = l \text{tr}(\boldsymbol{\Sigma}_2) \boldsymbol{\Sigma}_{1,i_1 i_2}$. This implies that the matrix structure of $\mathbb{E}(\mathbf{X}_t \mathbf{X}_t^\top)$ is determined by the column-wise variance-covariance matrix $\boldsymbol{\Sigma}_1$. Likewise, we have the second-order row-wise population moment $\mathbb{E}(\mathbf{X}_t^\top \mathbf{X}_t) = \{l \text{tr}(\boldsymbol{\Sigma}_1)\} \boldsymbol{\Sigma}_2$ and the analog row-wise view. By the strong factor assumption, we can show that $\mathbb{E}(\mathbf{X}_t \mathbf{X}_t^\top)$ and $\mathbb{E}(\mathbf{X}_t^\top \mathbf{X}_t)$ have approximately equal k_1 -dim and k_2 -dim leading eigenspaces of $\mathbf{R}\boldsymbol{\Psi}_A\mathbf{R}^\top$ and $\mathbf{C}\boldsymbol{\Psi}_B\mathbf{C}^\top$ respectively (Fan et al., 2020,

page 476), that is

$$\begin{aligned}\text{span}[\text{eig}\{\mathbb{E}(\mathbf{X}_t\mathbf{X}_t^\top), k_1\}] &= \text{span}\{\text{eig}(\boldsymbol{\Sigma}_1, k_1)\} \approx \text{span}(\mathbf{R}), \\ \text{span}[\text{eig}\{\mathbb{E}(\mathbf{X}_t^\top\mathbf{X}_t), k_2\}] &= \text{span}\{\text{eig}(\boldsymbol{\Sigma}_2, k_2)\} \approx \text{span}(\mathbf{C}).\end{aligned}$$

Therefore, approximating $\mathbb{E}(\mathbf{X}_t\mathbf{X}_t^\top)$ and $\mathbb{E}(\mathbf{X}_t^\top\mathbf{X}_t)$ by their second-order sample moments respectively, we have

$$\mathbb{E}(\mathbf{X}_t\mathbf{X}_t^\top) \approx \frac{1}{Tp_1p_2} \sum_{t=1}^T \mathbf{X}_t\mathbf{X}_t^\top =: \widehat{\mathbf{M}}_1; \quad \mathbb{E}(\mathbf{X}_t^\top\mathbf{X}_t) \approx \frac{1}{Tp_1p_2} \sum_{t=1}^T \mathbf{X}_t^\top\mathbf{X}_t =: \widehat{\mathbf{M}}_2.$$

Then we can obtain the following PCA estimators of loading matrices \mathbf{R} and \mathbf{C}

$$\widehat{\mathbf{R}} = \sqrt{p_1}\text{eig}(\widehat{\mathbf{M}}_1, k_1); \quad \widehat{\mathbf{C}} = \sqrt{p_2}\text{eig}(\widehat{\mathbf{M}}_2, k_2). \quad (6)$$

Thereafter we call $\widehat{\mathbf{R}}$ and $\widehat{\mathbf{C}}$ as sPCA estimators since our estimation is derived from the **separable covariance structure** of matrix-variate observations \mathbf{X}_t .

Remark 3. *Comparison with existing methods.* Estimation of loading matrices \mathbf{R} and \mathbf{C} shares common ground of combination of moment estimation and the truncated spectral decomposition under both the BiMFaM and the TeDFaM settings. Under the BiMFaM setting, the existing loading estimation methods are all mode-wise in the sense that the moment matrices are constructed directly row-wise or column-wise from the observed matrix variates. In detail, the spirit of α -PCA by Chen and Fan (2021) is to modify the matrix-variate observations by tuning sample means in their Subsection 2.2; the spirit of Yu et al. (2022) is to project the matrix observations along two modes in their Subsection 2.2; while the spirit of Wang et al. (2019) is to use the auto-correlation across matrix time series to construct the Box-Ljung type matrices that are identical to loadings in the sense of spanned column spaces in their Subsection 3.1. In contrast, the TeDFaM driven by CP-decomposition enjoys the separable covariance structure of the matrix-variate observation, and the resulting approximate equivalence of the spanned spaces of second-order population moments and loadings leads to spectral solutions of \mathbf{R} and \mathbf{C} naturally and intuitively.

Remark 4. *Factor scores and signal parts.* The sPCA estimators $\widehat{\mathbf{R}}$ and $\widehat{\mathbf{C}}$ derived under the TeDFaM (2) have the same form with the α -PCA estimator in Chen and Fan

(2021) when $\alpha = 0$, and the initial estimator in Yu et al. (2022) under the BiMFaM (3). Within the BiMFaM context, the resulting estimator of \mathbf{Z}_t is straight by multiplying $\widehat{\mathbf{R}}$ and $\widehat{\mathbf{C}}$ on the left and the right hand sides of \mathbf{X}_t , and accordingly \mathbf{S}_t instantly

$$\widetilde{\mathbf{Z}}_t = \frac{\widehat{\mathbf{R}}^\top \mathbf{X}_t \widehat{\mathbf{C}}}{p_1 p_2} \quad \text{and} \quad \widetilde{\mathbf{S}}_t = \frac{\widehat{\mathbf{R}} \widehat{\mathbf{R}}^\top \mathbf{X}_t \widehat{\mathbf{C}} \widehat{\mathbf{C}}^\top}{p_1 p_2}. \quad (7)$$

However, this is inapplicable under the TeDFaM setting because of presence of two mode-wise latent factors \mathbf{E}_t and \mathbf{F}_t .

3.2. Least Squares for Factor Scores

To obtain the factor scores $\widehat{\mathbf{Z}}_t$, $\widehat{\mathbf{E}}_t$, and $\widehat{\mathbf{F}}_t$ of the TeDFaM, we seek inspiration from the following minimization problem of the reconstruction error

$$\min_{\{\mathbf{Z}_t\}_{t=1}^T, \{\mathbf{E}_t\}_{t=1}^T, \{\mathbf{F}_t\}_{t=1}^T} \frac{1}{T p_1 p_2} \sum_{t=1}^T \|\mathbf{X}_t - \mathbf{R} \mathbf{Z}_t \mathbf{C}^\top - \mathbf{R} \mathbf{E}_t^\top - \mathbf{F}_t \mathbf{C}^\top\|_F^2,$$

where $\|\cdot\|_F$ is the Frobenius norm. Note that, we use the equations $p_1^{-1} \mathbf{R}^\top \mathbf{R} = \mathbf{I}_{k_1}$ and $p_2^{-1} \mathbf{C}^\top \mathbf{C} = \mathbf{I}_{k_2}$ directly to simplify the derivation in this subsection. By the fact that $\|\mathbf{A}\|_F^2 = \text{tr}(\mathbf{A} \mathbf{A}^\top)$, one may expand the objective function, and then take partial derivatives with respect to \mathbf{Z}_t , \mathbf{F}_t , and \mathbf{E}_t so as to obtain the normal equations. By some algebra, one may have system of equations as follows

$$\begin{cases} \mathbf{Z}_t = \frac{\mathbf{R}^\top \mathbf{X}_t \mathbf{C}}{p_1 p_2} - \frac{\mathbf{E}_t^\top \mathbf{C}}{p_2} - \frac{\mathbf{R}^\top \mathbf{F}_t}{p_1}, \\ (\mathbf{I}_{p_1} - \frac{\mathbf{R} \mathbf{R}^\top}{p_1}) (\mathbf{F}_t - \frac{\mathbf{X}_t \mathbf{C}}{p_2}) = \mathbf{0}_{p_1 \times k_2}, \\ (\mathbf{I}_{p_2} - \frac{\mathbf{C} \mathbf{C}^\top}{p_2}) (\mathbf{E}_t - \frac{\mathbf{X}_t^\top \mathbf{R}}{p_1}) = \mathbf{0}_{p_2 \times k_1}, \end{cases}$$

where $\mathbf{0}_{p \times q}$ represents the $p \times q$ matrix with zero entries. Note that $(\mathbf{I}_{p_1} - p_1^{-1} \mathbf{R} \mathbf{R}^\top)$ and $(\mathbf{I}_{p_2} - p_2^{-1} \mathbf{C} \mathbf{C}^\top)$ are orthogonal projection matrices with ranks $(p_1 - k_1)$ and $(p_2 - k_2)$, and their pseudoinverse matrices are themselves. Hence $\mathbf{F}_t - p_2^{-1} \mathbf{X}_t \mathbf{C} = (\mathbf{I}_{p_1} - p_1^{-1} \mathbf{R} \mathbf{R}^\top) \mathbf{0}_{p_1 \times k_2} = \mathbf{0}_{p_1 \times k_2}$ and $\mathbf{E}_t - p_1^{-1} \mathbf{X}_t^\top \mathbf{R} = (\mathbf{I}_{p_2} - p_2^{-1} \mathbf{C} \mathbf{C}^\top) \mathbf{0}_{p_2 \times k_1} = \mathbf{0}_{p_2 \times k_1}$ are the minimum norm solutions to the second and third linear systems respectively (Ben-Israel and Greville, 2003). Then by taking $\mathbf{F}_t = p_2^{-1} \mathbf{X}_t \mathbf{C}$ and $\mathbf{E}_t = p_1^{-1} \mathbf{X}_t^\top \mathbf{R}$ into the first equation system, we derive the solution $\mathbf{Z}_t = -(p_1 p_2)^{-1} \mathbf{R}^\top \mathbf{X}_t \mathbf{C}$. As a result, by adopting

the sPCA of \mathbf{R} and \mathbf{C} in the last subsection, the factor scores can be approximated by

$$\widehat{\mathbf{F}}_t = \frac{\mathbf{X}_t \widehat{\mathbf{C}}}{p_2}, \quad \widehat{\mathbf{E}}_t = \frac{\mathbf{X}_t^\top \widehat{\mathbf{R}}}{p_1}, \quad \widehat{\mathbf{Z}}_t = -\frac{\widehat{\mathbf{R}}^\top \mathbf{X}_t \widehat{\mathbf{C}}}{p_1 p_2}. \quad (8)$$

Note that the global latent factor $\widehat{\mathbf{Z}}_t$ of the TeDFaM is identical to $\widetilde{\mathbf{Z}}_t$ of the BiMFaM up to a sign. Accordingly, the estimated signal part of the TeDFaM is

$$\widehat{\mathbf{S}}_t = -\frac{\widehat{\mathbf{R}} \widehat{\mathbf{R}}^\top \mathbf{X}_t \widehat{\mathbf{C}} \widehat{\mathbf{C}}^\top}{p_1 p_2} + \frac{\widehat{\mathbf{R}} \widehat{\mathbf{R}}^\top \mathbf{X}_t}{p_1} + \frac{\mathbf{X}_t \widehat{\mathbf{C}} \widehat{\mathbf{C}}^\top}{p_2}. \quad (9)$$

3.3. Reconstruction Error Comparison

In this subsection, we compare the matrix reconstruction performance between the TeDFaM and the BiMFaM. We start from illustrating the relationship between image data and matrices. Given a set of possible gray levels or colors and a (rectangular) grid, a digital image attributes a gray value (i.e., brightness) or a color (i.e., hue, saturation and brightness) to each of the grid points or pixels (Suetens, 2017). Therefore, a 2D grayscale image can be represented as a matrix, in which the numbers of row and column represent the height and width of the grid, and each entry represents the pixel value ranging from 0 to 255. Typically, zero is taken to be black and 255 is taken to be white, that is, the larger the pixel value, the more intense brightness.

For the image data, a standard metric to measure the quality of reconstructed images compared with the original ones is the peak signal to noise ratio (PSNR), which is defined as

$$\text{PSNR} = 10 \log_{10} \frac{\|\mathbf{X}\|_{max}^2}{\|\mathbf{X} - \widehat{\mathbf{X}}\|_F^2 / p_1 p_2}, \quad (10)$$

where $\mathbf{X} = (x_{ij}) \in \mathbb{R}^{p_1 \times p_2}$ is the original image, $\widehat{\mathbf{X}} = (\widehat{x}_{ij}) \in \mathbb{R}^{p_1 \times p_2}$ is the reconstructed image, and $\|\mathbf{X}\|_{max}$ is the maximum of the absolute value of entries in \mathbf{X} (the maximum pixel value of the original image). The denominator $\|\mathbf{X} - \widehat{\mathbf{X}}\|_F^2 = \sum_{i=1}^{p_1} \sum_{j=1}^{p_2} (x_{ij} - \widehat{x}_{ij})^2$ characterizes the average of the square of the pixel differences between the reconstructed image and the original one. The greater the reconstructed image resembles the original one, the larger PSNR will be. But this can not guarantee that viewers will like the reconstructed image (Salomon, 2004). In addition, PSNR is dimensionless, and robust to small variations in the reconstructed image.

Note that for the t th image observation, the denominator of PSNR corresponds to the mean square error (MSE) of the TeDFaM and the BiMFaM respectively

$$\text{MSE}_{t,TeD} = \frac{1}{p_1 p_2} \|\mathbf{X}_t - \widehat{\mathbf{S}}_t\|_F^2, \quad \text{MSE}_{t,Bilinear} = \frac{1}{p_1 p_2} \|\mathbf{X}_t - \widetilde{\mathbf{S}}_t\|_F^2,$$

where $\widehat{\mathbf{S}}_t$ is the estimated signal part of the TeDFaM in equation (9) and $\widetilde{\mathbf{S}}_t$ is the estimated signal part of the BiMFaM in equation (7). Then the PSNR of the TeDFaM and the BiMFaM for the t th observation are

$$\text{PSNR}_{t,TeD} = 10 \log_{10} \frac{\|\mathbf{X}_t\|_{max}^2}{\text{MSE}_{t,TeD}}, \quad \text{PSNR}_{t,Bilinear} = 10 \log_{10} \frac{\|\mathbf{X}_t\|_{max}^2}{\text{MSE}_{t,Bilinear}}.$$

From the expression of PSNR, we can see that it is inversely proportional to MSE. Hence, greater resemblance between the original matrix/image observation and the reconstructed matrix/image implies larger PSNR and smaller MSE. Because of the use of the logarithm, PSNR is less sensitivity to changes in the MSE. Then we have the following proposition.

PROPOSITION 1. *For each matrix observation \mathbf{X}_t , $t \in [T]$, we have*

$$\text{PSNR}_{t,TeD} \geq \text{PSNR}_{t,Bilinear}. \quad (11)$$

or equivalently

$$\text{MSE}_{t,TeD} \leq \text{MSE}_{t,Bilinear}. \quad (12)$$

Proposition 1 guarantees the theoretical outperformance of the TeDFaM in terms of the matrix reconstruction error PSNR and MSE compared to the BiMFaM when using sPCA estimators. In addition, even other estimators (e.g. autoPCA, proPCA) are used for the BiMFaM, the TeDFaM still has better performance on the reconstruction error, which has been validated in the numerical studies. Note that from the formation of equation (10), both of PSNR and MSE can be used for general matrix observations not limited to image data.

3.4. Algorithm and Factor Number Estimation

When factor numbers k_1 and k_2 are known, the whole algorithm is summarized in Algorithm 1.

Algorithm 1 sPCA

-
- 1: **Input:** matrix observations $\{\mathbf{X}_t\}_{t=1}^T$, factor numbers k_1 and k_2 .
 - 2: compute the estimated loading matrices

$$\widehat{\mathbf{R}} = \sqrt{p_1} \text{eig}(\widehat{\mathbf{M}}_1, k_1) \text{ and } \widehat{\mathbf{C}} = \sqrt{p_2} \text{eig}(\widehat{\mathbf{M}}_2, k_2).$$

- 3: for $t \in [T]$, compute the estimated latent matrix factors and the signal part

$$\begin{aligned} \widehat{\mathbf{Z}}_t &= -\frac{\widehat{\mathbf{R}}^\top \mathbf{X}_t \widehat{\mathbf{C}}}{p_1 p_2}, \quad \widehat{\mathbf{F}}_t = \frac{\mathbf{X}_t \widehat{\mathbf{C}}}{p_2}, \quad \widehat{\mathbf{E}}_t = \frac{\mathbf{X}_t^\top \widehat{\mathbf{R}}}{p_1}, \\ \widehat{\mathbf{S}}_t &= -\frac{\widehat{\mathbf{R}} \widehat{\mathbf{R}}^\top \mathbf{X}_t \widehat{\mathbf{C}} \widehat{\mathbf{C}}^\top}{p_1 p_2} + \frac{\widehat{\mathbf{R}} \widehat{\mathbf{R}}^\top \mathbf{X}_t}{p_1} + \frac{\mathbf{X}_t \widehat{\mathbf{C}} \widehat{\mathbf{C}}^\top}{p_2}. \end{aligned}$$

- 4: **Output:** $\widehat{\mathbf{R}}, \widehat{\mathbf{C}}, \{\widehat{\mathbf{Z}}_t\}_{t=1}^T, \{\widehat{\mathbf{F}}_t\}_{t=1}^T, \{\widehat{\mathbf{E}}_t\}_{t=1}^T$, and $\{\widehat{\mathbf{S}}_t\}_{t=1}^T$.
-

If k_1 and k_2 are unknown, some estimators should be used to determine them before conducting the sPCA estimator. Hence, a general ratio-type estimator for the factor numbers are adopted. Denote $\widehat{\lambda}_1(\widehat{\mathbf{M}}_1) \geq \widehat{\lambda}_2(\widehat{\mathbf{M}}_1) \geq \dots \geq \widehat{\lambda}_{p_1}(\widehat{\mathbf{M}}_1) \geq 0$ as the ordered eigenvalues of $\widehat{\mathbf{M}}_1$ and k_{\max} as a given upper bound, the number of factors can be estimated as follows

$$\widehat{k}_1 = \arg \max_{1 \leq j \leq k_{\max}} \frac{\widehat{\lambda}_j(\widehat{\mathbf{M}}_1)}{\widehat{\lambda}_{j+1}(\widehat{\mathbf{M}}_1)}, \quad (13)$$

where \widehat{k}_2 can be defined similarly. This ratio-type estimator is widely used in factor models including the vector case and the matrix case (Lam and Yao, 2012; Yu et al., 2022). The consistency of the estimation is proved in the next section.

4. Asymptotic Properties

4.1. Assumptions

Before presenting the theoretical results, we need to provide the following assumptions, which are similar to those for the BiMFaM (Chen and Fan, 2021; Yu et al., 2022), and can be regarded as extensions of those used in high-dimensional vector factor models (Stock and Watson, 2002; Bai, 2003).

Assumption 1. *α -mixing:* the vectorized factor processes $\{\text{vec}(\mathbf{Z}_t)\}, \{\text{vec}(\mathbf{F}_t)\}, \{\text{vec}(\mathbf{E}_t)\}$, and the noise process $\{\text{vec}(\mathbf{e}_t)\}$ are α -mixing.

For a vector process $\{\mathbf{u}_t\}$, it is said to be α -mixing, if $\sum_{h=1}^{\infty} \alpha(h)^{1-2/\gamma} < \infty$ for some $\gamma > 2$, where $\alpha(h) = \sup_i \sup_{A \in \mathcal{C}_{-\infty}^i, B \in \mathcal{C}_{i+h}^{\infty}} |P(A \cap B) - P(A)P(B)|$ with \mathcal{C}_i^j as the σ -field generated by $\{\mathbf{u}_t : i \leq t \leq j\}$. The α -mixing condition of a process tells us when the variables are sufficiently far apart, they are asymptotic independent (Francq and Zakoian, 2019, Appendix A.3).

Assumption 2 *Common factors*: assume k_1 and k_2 are fixed, for any $t \in [T], i \in [p_1], j \in [p_2], u \in [k_1]$ and $v \in [k_2]$, there exists a positive constant m such that $\mathbb{E}(Z_{t,uv}^4) \leq m$, $\mathbb{E}(F_{t,iv}^4) \leq m$, $\mathbb{E}(E_{t,ju}^4) \leq m$ and

$$\begin{aligned} \frac{1}{T} \sum_{t=1}^T \mathbf{Z}_t \mathbf{Z}_t^\top &\xrightarrow{a.s.} \boldsymbol{\Sigma}_{Z1}, & \frac{1}{T} \sum_{t=1}^T \mathbf{Z}_t^\top \mathbf{Z}_t &\xrightarrow{a.s.} \boldsymbol{\Sigma}_{Z2}, \\ \frac{1}{Tp_1} \sum_{t=1}^T \mathbf{F}_t^\top \mathbf{F}_t &\xrightarrow{a.s.} \boldsymbol{\Sigma}_F, & \frac{1}{Tp_2} \sum_{t=1}^T \mathbf{E}_t^\top \mathbf{E}_t &\xrightarrow{a.s.} \boldsymbol{\Sigma}_E, \end{aligned}$$

where $\boldsymbol{\Sigma}_{Z1} \in \mathbb{R}^{k_1 \times k_1}$, $\boldsymbol{\Sigma}_{Z2} \in \mathbb{R}^{k_2 \times k_2}$, $\boldsymbol{\Sigma}_F \in \mathbb{R}^{k_2 \times k_2}$ and $\boldsymbol{\Sigma}_E \in \mathbb{R}^{k_1 \times k_1}$ are positive definite matrices. Denote $\boldsymbol{\Sigma}_1 = \boldsymbol{\Sigma}_E + \boldsymbol{\Sigma}_{Z1}$ and $\boldsymbol{\Sigma}_2 = \boldsymbol{\Sigma}_F + \boldsymbol{\Sigma}_{Z2}$, assume $\boldsymbol{\Sigma}_1$ and $\boldsymbol{\Sigma}_2$ have spectral decompositions $\boldsymbol{\Sigma}_1 = \boldsymbol{\Gamma}_1 \boldsymbol{\Lambda}_1 \boldsymbol{\Gamma}_1^\top$ and $\boldsymbol{\Sigma}_2 = \boldsymbol{\Gamma}_2 \boldsymbol{\Lambda}_2 \boldsymbol{\Gamma}_2^\top$ respectively, where the diagonal elements of $\boldsymbol{\Lambda}_1$ and $\boldsymbol{\Lambda}_2$ are distinct and arranged in decreasing order.

First, Assumption 2 assumes that the matrix factor has bounded fourth-order moment. Next, it assumes the second-order sample moment of the matrix factors converge to some positive definite matrix, which can be derived under the α -mixing Assumption 1, see (Athreya and Lahiri, 2006, Chapter 16) and (Francq and Zakoian, 2019, Appendix A.3.) for more details. At last, the assumption of distinct and decreasing eigenvalues of $\boldsymbol{\Sigma}_1$ and $\boldsymbol{\Sigma}_2$ result in unique eigen-decomposition and identifiable eigenvectors. Assumption 2 is an extension of that in (Yu et al., 2022) with extra row-wise and column-wise factors.

Assumption 3 *Loading matrices*: there exist positive constants \bar{r} and \bar{c} such that $\|\mathbf{R}\|_{max} \leq \bar{r}$, $\|\mathbf{C}\|_{max} \leq \bar{c}$. As $\min\{p_1, p_2\} \rightarrow \infty$, we have $\|p_1^{-1} \mathbf{R}^\top \mathbf{R} - \mathbf{I}_{k_1}\| \rightarrow 0$ and $\|p_2^{-1} \mathbf{C}^\top \mathbf{C} - \mathbf{I}_{k_2}\| \rightarrow 0$, where $\|\cdot\|$ is the L_2 -norm of a matrix.

Assumption 3 is not only used as model identification conditions, but also guarantee that our model belongs to the strong factor regime, which means that the factors are pervasively shared by entries of the observations, and the signal part has spiked eigenval-

ues relative to the noise part (Stock and Watson, 2002; Lam and Yao, 2011; Fan et al., 2013; Chen et al., 2020c).

Assumption 4 *Correlation*: assume $\{\mathbf{e}_t\}$ is a temporal independent serie, $\{\mathbf{Z}_t\}$, $\{\mathbf{F}_t\}$ and $\{\mathbf{E}_t\}$ are cross-sectional independent series. For any $s, t \in [T]$, $i, i_1, i_2 \in [p_1]$, $j, j_1, j_2 \in [p_2]$, $u \in [k_1]$ and $v \in [k_2]$, there exists a positive constant m such that

- (a) $\mathbb{E}(\mathbf{e}_t) = \mathbf{0}$ and $\mathbb{E}(e_{t,ij}^8) \leq m$.
- (b) $\sum_{i_1=1}^{p_1} \sum_{j_1=1}^{p_2} |\mathbb{E}(e_{t,i_1j_1} e_{t,i_2j_2})| \leq m$.
- (c) $\sum_{i_1, i_2=1}^{p_1} \sum_{j_1, j_2=1}^{p_2} |\text{cov}(e_{t,i_1j_1} e_{t,i_2j_2}, e_{t,i_1j_1'} e_{t,i_2j_2'})| \leq m$.
- (d) $\sum_{t=1}^T |\mathbb{E}(F_{t,iv} F_{s,iv})| \leq m$, $\sum_{t=1}^T |\mathbb{E}(E_{t,ju} E_{s,ju})| \leq m$, $\sum_{t=1}^T |\mathbb{E}(Z_{t,uv} Z_{s,uv})| \leq m$.

Assumption 4 focus on the cross-sectional correlation of the noise matrix \mathbf{e}_t , and the temporal correlation of factor matrices \mathbf{Z}_t , \mathbf{F}_t and \mathbf{E}_t . First, Assumption 4.1 assume the matrix noise has zero expectation and bounded eighth-order moment of each element. Second, Assumption 4.2 illustrates that the correlation across different elements of \mathbf{e}_t is weak. Next, Assumption 4.3 shows that the correlation across different elements of $\mathbf{e}_t \circ \mathbf{e}_t \in \mathbb{R}^{p_1 \times p_2 \times p_1 \times p_2}$ is weak, where \circ is the outer product. At last, Assumption 4.4 assumes that the temporal correlation of the same cross-sectional element of \mathbf{Z}_t , \mathbf{F}_t and \mathbf{E}_t are weak. In a word, we assume the correlation in the noise part and the factors are weak, and the independent matrix observations, as a special case, satisfy Assumption 4.

Assumption 5 *Central limit theorems*:

- (a) for $i \in [p_1]$,

$$\frac{1}{\sqrt{T}} \sum_{t=1}^T \mathbf{Z}_t \mathbf{F}_{t,i} \xrightarrow{d} N(\mathbf{0}, \mathbf{V}_{1i}), \quad \text{where } \mathbf{V}_{1i} = \lim_{T \rightarrow \infty} \frac{1}{T} \sum_{s,t} \mathbb{E}(\mathbf{Z}_t \mathbf{F}_{t,i} \mathbf{F}_{s,i}^\top \mathbf{Z}_s^\top);$$

- (b) for $j \in [p_2]$,

$$\frac{1}{\sqrt{T}} \sum_{t=1}^T \mathbf{Z}_t^\top \mathbf{E}_{t,j} \xrightarrow{d} N(\mathbf{0}, \mathbf{V}_{2j}), \quad \text{where } \mathbf{V}_{2j} = \lim_{T \rightarrow \infty} \frac{1}{T} \sum_{s,t} \mathbb{E}(\mathbf{Z}_t^\top \mathbf{E}_{t,j} \mathbf{E}_{s,j}^\top \mathbf{Z}_s^\top).$$

Assumption 5 is useful when derive the asymptotic distribution of the estimated loading matrices. Under Assumptions 1-4, Assumption 5 can be derived by central limit theorem for α -mixing processes Athreya and Lahiri (2006); Francq and Zakoian (2019). Assumption 5 is distinct with the corresponding condition used in BiMFaM in that the main term are changed due to the incorporation of row-wise and column-wise factors.

4.2. Asymptotic Properties

Note that Assumption 3 only assure the column space uniqueness up to an orthogonal rotation, we prove that there exists asymptotic orthogonal matrices $\widehat{\mathbf{H}}_1$ and $\widehat{\mathbf{H}}_2$ such that $\widehat{\mathbf{R}}$ is a consistency estimator of $\mathbf{R}\widehat{\mathbf{H}}_1$, and $\widehat{\mathbf{C}}$ is a consistency estimator of $\mathbf{C}\widehat{\mathbf{H}}_2$. Then the convergence rates of $\widehat{\mathbf{R}}$ and $\widehat{\mathbf{C}}$ are shown in terms of Frobenius norm in Theorem 1 as follows.

THEOREM 1. *Suppose T , p_1 and p_2 tend to infinity, k_1 and k_2 are fixed. If Assumptions 1-4 hold, then there exist asymptotic orthogonal matrices $\widehat{\mathbf{H}}_1$ and $\widehat{\mathbf{H}}_2$ such that*

$$\frac{1}{p_1} \|\widehat{\mathbf{R}} - \mathbf{R}\widehat{\mathbf{H}}_1\|_F^2 = O_p\left(\frac{1}{T} + \frac{1}{p_1^2}\right), \text{ and } \frac{1}{p_2} \|\widehat{\mathbf{C}} - \mathbf{C}\widehat{\mathbf{H}}_2\|_F^2 = O_p\left(\frac{1}{T} + \frac{1}{p_2^2}\right).$$

The convergence rate of $\widehat{\mathbf{R}}$ ($\widehat{\mathbf{C}}$) in theorem 1 is same to the high-dimensional vector factor models in Bai (2003) with T samples of size p_1 or p_2 . For the BiMFaM, the convergence rates of the autoPCA estimators in Wang et al. (2019) are $O_p(\frac{1}{T})$, and the convergence rates for α -PCA estimators are $O_p(\frac{1}{Tp_2} + \frac{1}{p_1^2})$ and $O_p(\frac{1}{Tp_1} + \frac{1}{p_2^2})$ respectively, which are identical to the vector factor models with Tp_2 or Tp_1 samples of size p_1 or p_2 (Yu et al., 2022). Hence, the TeDFaM improves the reconstruction performance at the cost of convergence rate when $Tp_2 = o(p_1^2)$ and $Tp_1 = o(p_2^2)$. The difference is due to the incorporation of row and column effects besides the interaction one.

With the above consistency, we can derive the asymptotic distribution of the estimated loading matrices. Because the row sizes of \mathbf{R} and \mathbf{C} tend to infinity, we will provide the asymptotic distribution row-wisely as shown in the following Theorem 2.

THEOREM 2. *Suppose T , p_1 and p_2 tend to infinity, k_1 and k_2 are fixed. If Assumptions 1-5 hold, then*

(a) for $i \in [p_1]$, we have

$$\begin{cases} \sqrt{T}(\widehat{\mathbf{R}}_{i\cdot} - \widehat{\mathbf{H}}_1^\top \mathbf{R}_{i\cdot}) \xrightarrow{d} N(\mathbf{0}, \mathbf{\Lambda}_1^{-1} \mathbf{\Gamma}_1^\top \mathbf{V}_{1i} \mathbf{\Gamma}_1 \mathbf{\Lambda}_1^{-1}), & T = o_p(p_1^2), \\ \widehat{\mathbf{R}}_{i\cdot} - \widehat{\mathbf{H}}_1^\top \mathbf{R}_{i\cdot} = O_p(\frac{1}{p_1}), & p_1^2 = O_p(T); \end{cases}$$

(b) for $j \in [p_2]$, we have

$$\begin{cases} \sqrt{T}(\widehat{\mathbf{C}}_{j\cdot} - \widehat{\mathbf{H}}_2^\top \mathbf{C}_{j\cdot}) \xrightarrow{d} N(\mathbf{0}, \mathbf{\Lambda}_2^{-1} \mathbf{\Gamma}_2^\top \mathbf{V}_{2j} \mathbf{\Gamma}_2 \mathbf{\Lambda}_2^{-1}), & T = o_p(p_2^2), \\ \widehat{\mathbf{C}}_{j\cdot} - \widehat{\mathbf{H}}_2^\top \mathbf{C}_{j\cdot} = O_p(\frac{1}{p_2}), & p_2^2 = O_p(T). \end{cases}$$

Theorem 2 shows that the estimated loading matrix can reach asymptotic normality when p_1 and p_2 are sufficiently large. Even if it was not the case, the estimated loading matrices are still consistent regardless of the limit relationship between T and $\{p_d\}_{d=1}^2$. After obtaining the theoretic properties of loading matrices, we turn to the consistency of the estimated signal part. Because the size of \mathbf{S}_t tends to infinity, we will provide its consistency element-wisely. The (i, j) th elements of \mathbf{S}_t and $\widehat{\mathbf{S}}_t = \widehat{\mathbf{X}}_t$ are denoted as

$$S_{t,ij} = \mathbf{R}_{i\cdot}^\top \mathbf{Z}_t \mathbf{C}_{j\cdot} + \mathbf{R}_{i\cdot}^\top \mathbf{E}_{t,j\cdot} + \mathbf{F}_{t,i\cdot}^\top \mathbf{C}_{j\cdot} \quad \text{and} \quad \widehat{S}_{t,ij} = \widehat{\mathbf{R}}_{i\cdot}^\top \widehat{\mathbf{Z}}_t \widehat{\mathbf{C}}_{j\cdot} + \widehat{\mathbf{R}}_{i\cdot}^\top \widehat{\mathbf{E}}_{t,j\cdot} + \widehat{\mathbf{F}}_{t,i\cdot}^\top \widehat{\mathbf{C}}_{j\cdot},$$

then we provide the consistency of $\widehat{S}_{t,ij}$ in the following theorem.

THEOREM 3. *Suppose T , p_1 and p_2 tend to infinity, k_1 and k_2 are fixed. If Assumptions 1-4 hold, then we have*

$$|\widehat{S}_{t,ij} - S_{t,ij}| = O_p\left(\frac{1}{\sqrt{T}} + \frac{1}{\sqrt{p_1}} + \frac{1}{\sqrt{p_2}}\right).$$

Similar to the difference on the convergence rates of loading matrices, the convergence rate of the signal part for the TeDFaM is slower than that of the BiMFaM. But as shown in proposition 1, the TeDFaM improves the reconstruction performance. Theorems 1-3 are proved with fixed factor numbers k_1 and k_2 . If the factor numbers are unknown, the ratio-type estimation in equation (13) is used and its consistency is given in Theorem 4 below.

THEOREM 4. *Suppose T , p_1 and p_2 tend to infinity, k_1 and k_2 are fixed. If Assumptions 1-4 hold, then we have*

$$P(\widehat{k}_1 \neq k_1) \rightarrow 0 \quad \text{and} \quad P(\widehat{k}_2 \neq k_2) \rightarrow 0.$$

Theorem 4 illustrates that if k_{max} is big enough, the factor numbers can be estimated consistently. Because our estimation has same form with the initial estimator in Yu et al. (2022) and the α -PCA estimator in Chen and Fan (2021) with $\alpha = -1$, the ratio-type estimator will provide the same factor numbers estimation for the TeDFaM and the BiMFaM.

5. Numerical Studies

In this section, we conduct simulations to evaluate the finite sample performance of the proposed TeDFaM with the sPCA estimator. The simulation settings are introduced in Subsection 5.1 with four different simulation scenarios. The simulation results are reported in Subsection 5.2, including measurements used for assessments, the estimation errors of estimated loading matrices, signal parts and the matrix reconstruction, and the asymptotic normality demonstration.

5.1. Simulation Settings

The simulation data is generated with factor numbers $k_1 = k_2 = 3$. The specific data generating procedure is as follows. First, the loading matrix \mathbf{R} is taken as the $\sqrt{p_1}$ times the first k_1 left singular vectors of the SVD decomposition on the matrix with standard normal elements, and the loading matrix \mathbf{C} is generated similarly. Second, we generate \mathbf{Z}_t , \mathbf{E}_t and \mathbf{F}_t from the vector auto-regression models as follows

$$\begin{aligned}\text{vec}(\mathbf{Z}_t) &= \phi \text{vec}(\mathbf{Z}_{t-1}) + \sqrt{1 - \phi^2} \mathbf{u}_t, \\ \text{vec}(\mathbf{F}_t) &= \psi \text{vec}(\mathbf{F}_{t-1}) + \sqrt{1 - \psi^2} \boldsymbol{\xi}_t, \\ \text{vec}(\mathbf{E}_t) &= \gamma \text{vec}(\mathbf{E}_{t-1}) + \sqrt{1 - \gamma^2} \boldsymbol{\eta}_t,\end{aligned}$$

where $\mathbf{u}_t \sim N(\mathbf{0}, \mathbf{I}_{k_1 k_2})$, $\boldsymbol{\xi}_t \sim N(\mathbf{0}, \mathbf{I}_{p_1 k_2})$, $\boldsymbol{\eta}_t \sim N(\mathbf{0}, \mathbf{I}_{p_2 k_1})$, and the entries of initial values of $\text{vec}(\mathbf{Z}_t)$, $\text{vec}(\mathbf{F}_t)$ and $\text{vec}(\mathbf{E}_t)$ are standard normal. The coefficients ϕ , ψ and γ control the temporal correlation of the matrix factors. At last, we generate $\mathbf{e}_t \sim MN(\mathbf{0}; \mathbf{U}_e, \mathbf{V}_e)$, where \mathbf{U}_e and \mathbf{V}_e both have 1's on the diagonal, while off-diagonal elements are $1/p_1$ and $1/p_2$ respectively. We consider four different scenarios for simulations.

Scenario I: (Uncorrelated & TeDFaM) Let $(\phi, \psi, \gamma) = (0, 0, 0)$, which means the matrix factor series are temporal uncorrelated, and generate data from the TeDFaM (2).

Scenario II: (Uncorrelated & BiMFaM) Let $(\phi, \psi, \gamma) = (0, 0, 0)$, which means the matrix factor series are temporal uncorrelated, and generate data from the BiMFaM, i.e., only including the bilinear part.

Scenario III: (Correlated & TeDFaM) Let $(\phi, \psi, \gamma) = (0.6, 0.8, 0.8)$, which means the matrix factor series are temporal correlated, and generate data from the TeDFaM (2).

Scenario IV: (Correlated & BiMFaM) Let $(\phi, \psi, \gamma) = (0.6, 0.8, 0.8)$, which means the matrix factor series are temporal correlated, and generate data from the BiMFaM.

5.2. Performance Measurements and Simulation Results

First, we consider 6 sizes of (T, p_1, p_2) , which are $(20, 50, 100)$, $(20, 100, 100)$, $(50, 20, 50)$, $(50, 100, 100)$, $(100, 20, 50)$ and $(100, 50, 100)$. Four methods, i.e., the sPCA estimator for TeDFaM, the autoPCA (Wang et al., 2019), the α -PCA with $\alpha = -1$ (Chen and Fan, 2021), and the proPCA for BiMFaM (Yu et al., 2022), are used for comparing the consistency of loading matrices and the signal part, and the reconstruction error.

Measurements: For loading matrices, the following measurements are used

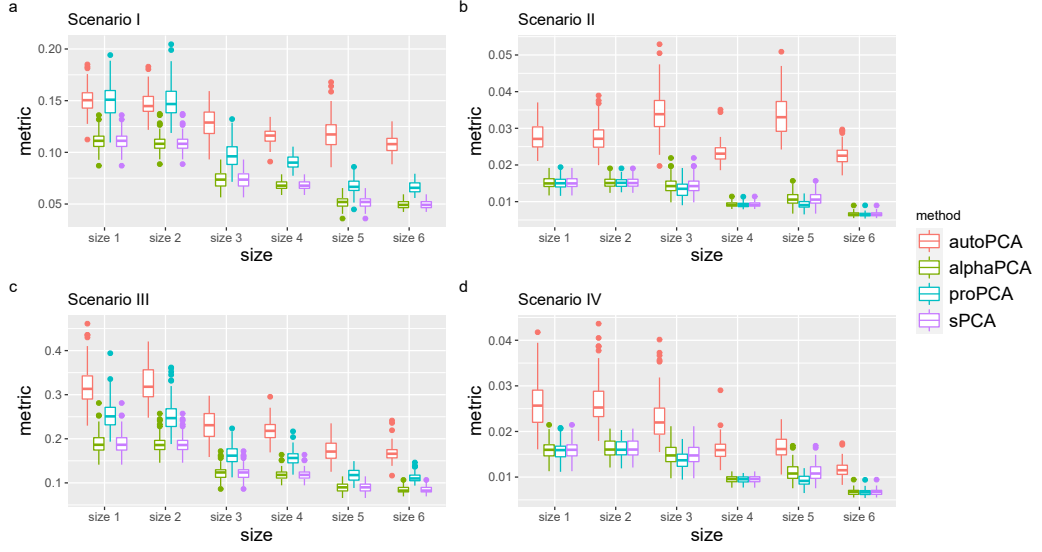
$$\begin{aligned} \mathcal{D}(\widehat{\mathbf{R}}, \mathbf{R}) &= \|\widehat{\mathbf{R}}(\widehat{\mathbf{R}}^\top \widehat{\mathbf{R}})^{-1} \widehat{\mathbf{R}}^\top - \mathbf{R}(\mathbf{R}^\top \mathbf{R})^{-1} \mathbf{R}^\top\|_2, \\ \mathcal{D}(\widehat{\mathbf{C}}, \mathbf{C}) &= \|\widehat{\mathbf{C}}(\widehat{\mathbf{C}}^\top \widehat{\mathbf{C}})^{-1} \widehat{\mathbf{C}}^\top - \mathbf{C}(\mathbf{C}^\top \mathbf{C})^{-1} \mathbf{C}^\top\|_2, \end{aligned}$$

where $\mathcal{D}(\widehat{\mathbf{R}}, \mathbf{R})$ and $\mathcal{D}(\widehat{\mathbf{C}}, \mathbf{C})$ characterize the distance of the column space between the estimation and the true value. The consistency of the estimated signal part is gauged by the following root mean square error (RMSE) measurement

$$\text{RMSE}_S = \sqrt{\frac{1}{Tp_1p_2} \sum_{t=1}^T \|\widehat{\mathbf{S}}_t - \mathbf{S}_t\|_F^2},$$

and reconstruction error are gauged by the following RMSE and PSNR measurements

$$\text{RMSE}_X = \sqrt{\frac{1}{Tp_1p_2} \sum_{t=1}^T \|\widehat{\mathbf{S}}_t - \mathbf{X}_t\|_F^2}, \quad \text{PSNR} = \frac{1}{T} \sum_{t=1}^T \text{PSNR}_t.$$

**Fig. 3.** Consistency of \mathbf{R}

Estimation errors: The average values of the above measurements for 100 replications are reported in Figures 3-7. As we can see from Figures 3 and 4, the estimation for the TeDFaM is same to the α -PCA with $\alpha = -1$ of the BiMFaM, so their results of $\mathcal{D}(\widehat{\mathbf{R}}, \mathbf{R})$ and $\mathcal{D}(\widehat{\mathbf{C}}, \mathbf{C})$ are identical regardless of the generation model. But the proPCA method performs worse for the TeDFaM (Scenario I and Scenario III) and better for the BiMFaM (Scenario II and Scenario IV), which is in accordance with the results in Yu et al. (2022). As for the autoPCA method, its poor performance is due to its inapplicability of these scenarios. From Figures 5 and 7, we can see that the sPCA performs worse in terms of the estimation error of the signal part with the BiMFaM as the generation model, but the reconstruction performance of the sPCA is better than other methods regardless of generation models (smaller RMSE and larger PSNR).

Asymptotic normality: The asymptotic normality of $\widehat{\mathbf{R}}$ as well as its asymptotic covariance matrix are evaluated. To simplify the computation of the asymptotic covariance matrix, Scenario I is adopted and some simple algebra gives that the asymptotic covariance matrix of $\widehat{\mathbf{R}}_i$ is $k_2/(k_2 + 1)^2 \mathbf{I}_{k_1}$. We set $T = 100$, $(p_1, p_2) = (150, 150)$, and shows the histogram of the third element of $(k_2 + 1)\sqrt{T/k_2}(\widehat{\mathbf{R}}_1 - \widehat{\mathbf{H}}_1^\top \mathbf{R}_1)$ with 1000

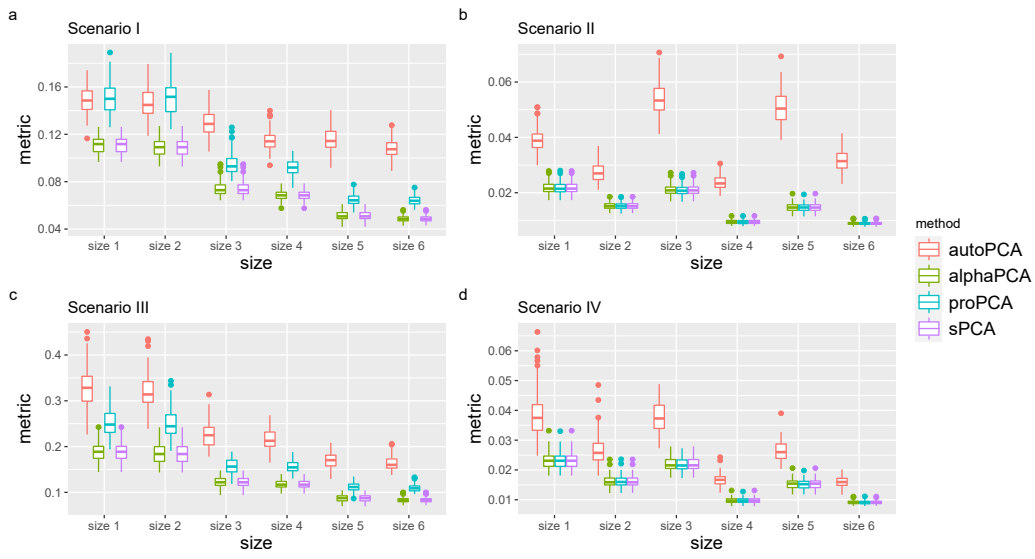


Fig. 4. Consistency of C

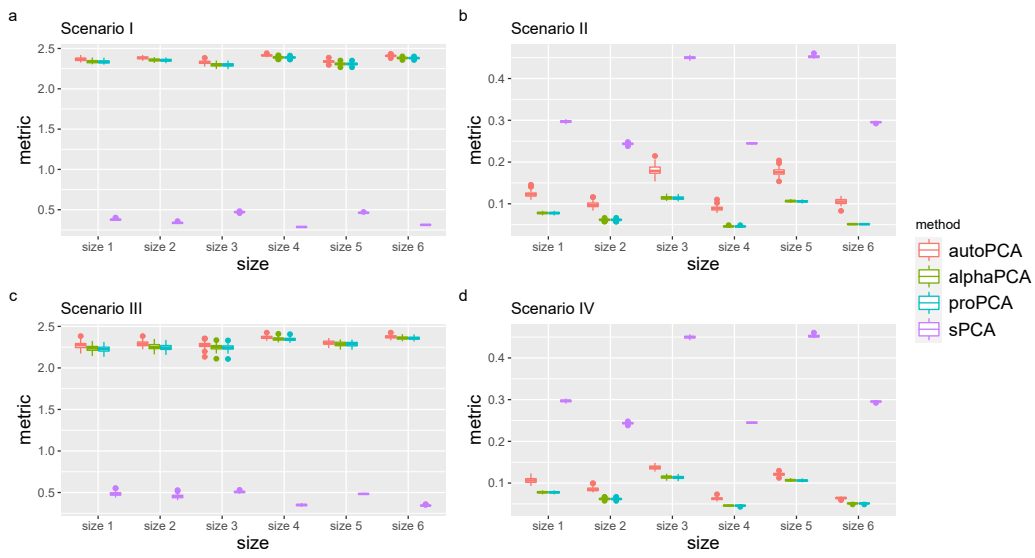


Fig. 5. Consistency of the signal part

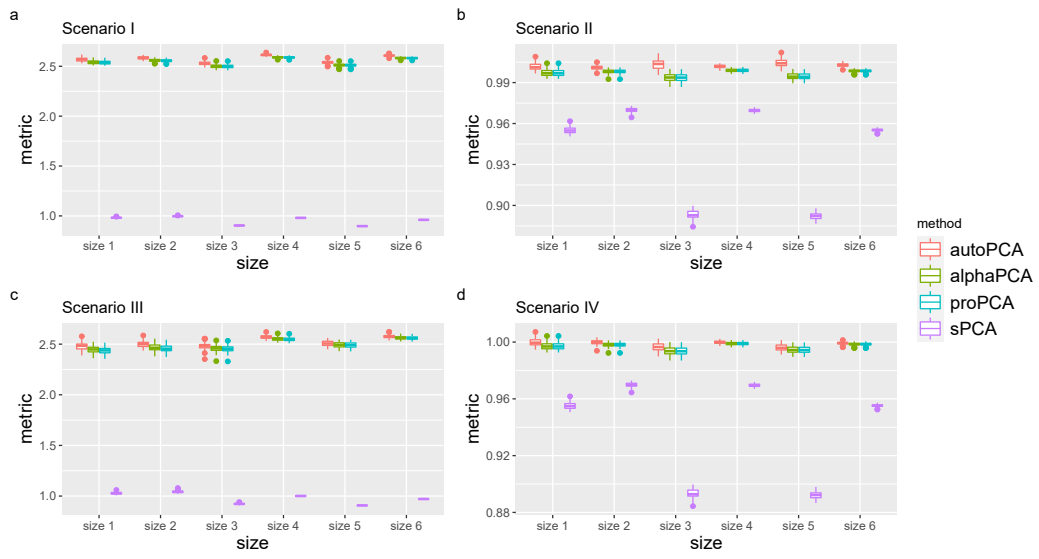


Fig. 6. Results of the RMSE

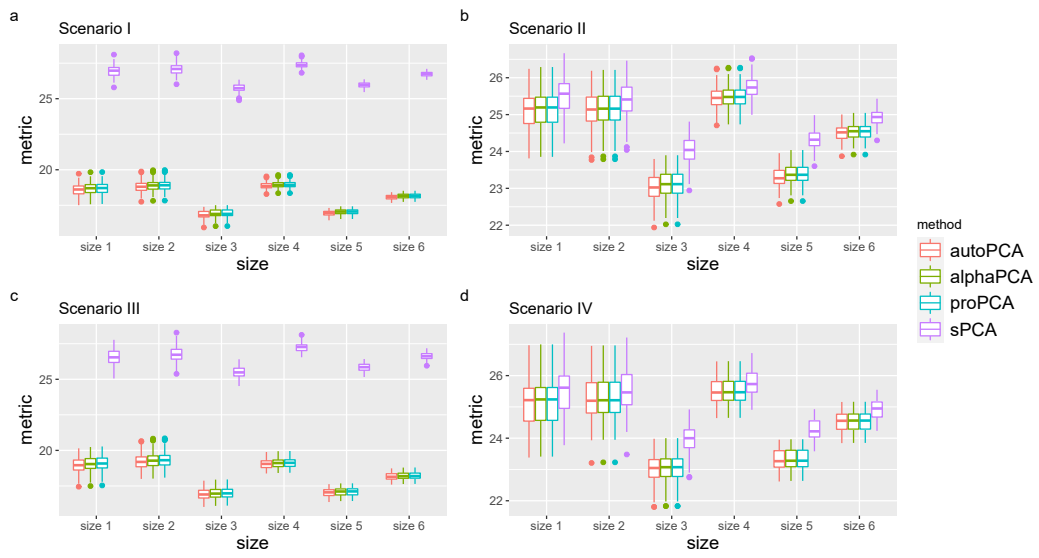


Fig. 7. Results of the PSNR

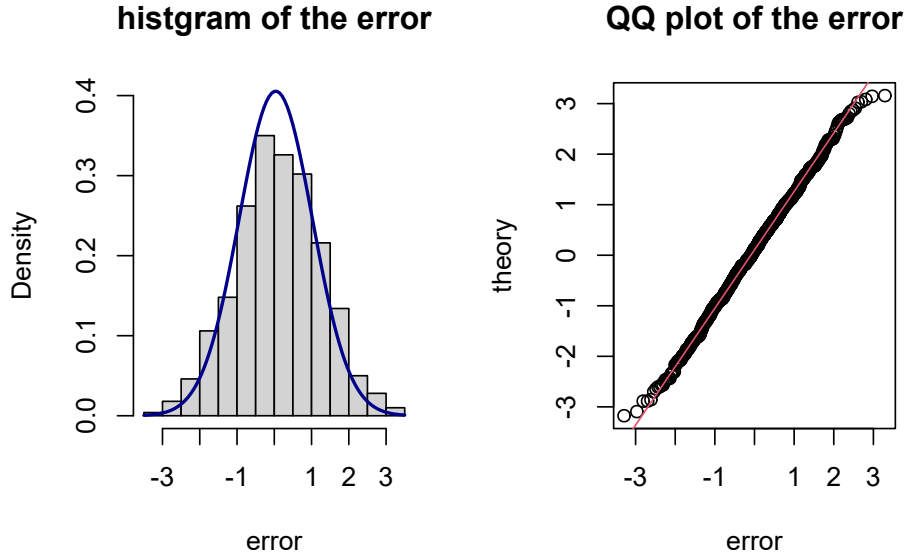


Fig. 8. Asymptotic Normality of $\hat{\mathbf{R}}_{13}$

replications in Figure 8, where the curve is the probability density function of standard normal distribution. The right plot of Figure 8 shows the QQ plot satisfying the normal distribution, and the p -value of the Shapiro-Wilk test is 0.4243.

6. Real Data Analysis

6.1. CT image dataset about COVID-19

Nucleic acid detection, antibodies detection via blood testing and computed tomography (CT) imaging are the most common tests method for detection of COVID-19. At the early outbreak of COVID-19, due to the shortage of test kits, CT and other chest imaging techniques have been named as an important way for diagnosing COVID-19 (Yang et al., 2020). The gray-scale image data can be regarded as matrix data. In this section, the proposed method is applied to the COVID-CT dataset collected by Yang et al. (2020), which contains 714 CT images of COVID-19 with values between 0 and 1. Each image has been resized to 150×150 , hence we have $T = 714$, $p_1 = 150$ and $p_2 = 150$. The estimated signal part can be seen as the reconstruction of the original image. To evaluate

Table 1. The result of the RMSE for different choice of k_1 and k_2 .

Method	(5, 5)	(15, 15)	(25, 25)	(35, 35)	(45, 45)
autoPCA	0.20092	0.13467	0.10970	0.09489	0.08358
α -PCA	0.19069	0.12377	0.09755	0.08143	0.06980
proPCA	0.18986	0.12303	0.09691	0.08097	0.06949
sPCA	0.12464	0.07824	0.05791	0.04556	0.03691
AE-1	0.34028	0.34035	0.34031	0.34044	0.34043
AE-5	0.34026	0.34030	0.34029	0.34031	0.34030
CAE	0.33797	0.33798	0.33795	0.33782	0.33777

the performance of the matrix reconstruction, the intra sample RMSE and PSNR are used as the measurement under different factor numbers.

Other than the four PCA type methods, i.e., the autoPCA, the α -PCA and the proPCA for the BiMFaM, and the sPCA for the TeDFaM, the autoencoder (AE) method is used as well (Hinton and Salakhutdinov, 2006; Fan et al., 2021). For the latent feature dimension of the AE, we set the neuron numbers of the 1 hidden layers network AE-1 and the 5 hidden layers network AE-5 as k_1 and $(256, 128, k_1, 128, 256)$ respectively. We use the whole sample size as the batch size, and conduct 500 epochs. In addition, we use a convolutional autoencoder (CAE) of 8 hidden layer with k_1 as the neuron numbers of the central fully connected bottleneck layer (Guo et al., 2017). We use the 32 as the batch size, and conduct 50 epochs. The results are shown in Tables 1 and 2, from which we can see that our method has better performance for all choice of k_1 and k_2 . As for the AE/CAE approach, all the PCA type methods outperform it, which probably be because the sample size is too small for the deep learning methods (underfitting), and the the vectorized images input cause the structural information loss, while the matrix factor models have much less parameters and adopt the matrix structure directly. In addition, we also compare with the refined TCPD method in Chang et al. (2021) with time lag $K = 1$, CP rank $d = 1$, and random selected linear combination. The RMSE and PSNR results are 0.33393 and 9.83213 respectively. We can see that, although CP type model may compress the data more effectively, its reconstruction performance is less satisfactory.

Table 2. The result of the PSNR for different choice of k_1 and k_2 .

Method	(5, 5)	(15, 15)	(25, 25)	(35, 35)	(45, 45)
autoPCA	14.14984	17.66109	19.4595	20.75663	21.91098
α -PCA	14.62127	18.38889	20.5233	22.19565	23.6577
proPCA	14.6597	18.43343	20.57564	22.24374	23.6945
sPCA	18.30163	22.47878	25.31639	27.67725	29.8249
AE-1	9.51019	9.50850	9.50941	9.50603	9.50610
AE-5	9.51072	9.50966	9.51016	9.50959	9.50978
CAE	9.57029	9.57010	9.57089	9.57421	9.57552

6.2. Multinational macroeconomic indices

In this subsection, we analyze the multinational macroeconomic indices data set, which is similar to the data set used in Chen and Fan (2021) and Yu et al. (2022), and is collected from OECD. It contains 10 quarterly macroeconomic indices of 14 countries from 2000.Q1 to 2018.Q2 for 74 quarters. The countries include United States, Canada, New Zealand, Australia, Norway, Ireland, Denmark, United Kingdom, Finland, Sweden, France, Netherlands, Austria and Germany. The indices consist of four groups, which are the production group (P:TIEC, P:TM, GDP), the consumer price group (CPI:FOOD, CPI:ENER, CPI:TOT), the money market group (IR:Long, IR:SHORT), and the international trade group (IT:EXP, IT:IM).

The data has been preprocessed similar to that of Chen and Fan (2021) as follows. For the production and the international trade groups, the original univariate time series are transformed by taking the first difference of the logarithm. For the consumer price group, the original univariate time series are transformed by taking the second difference of the logarithm. For the money market group, the original univariate time series are transformed by taking the first difference. Hence, after centralizing the matrix-variate series to eliminate the mean effects, we have observations with $T = 72$, $p_1 = 14$ and $p_2 = 10$. Four methods, i.e., the autoPCA, the α -PCA and the proPCA for the BiMFaM, and the sPCA for the TeDFaM are adopted in accordance with simulation studies.

Factor loadings and clustering: we use $k_1 = 3$ and $k_2 = 4$ to fit the model. For the sake of interpretability, the varimax rotation is applied on the loading matrices, and

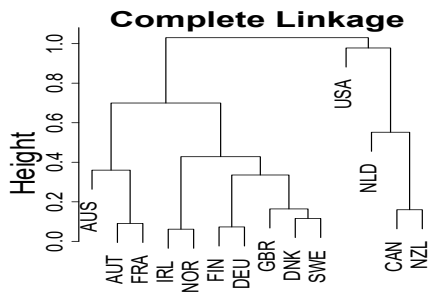
Table 3. The estimation of the row factor loading matrix \mathbf{R} .

Method	Factor	AUS	AUT	CAN	DNK	FIN	FRA	DEU	IRL	NLD	NZL	NOR	SWE	GBR	USA
autoPCA	1	-6	0	0	-6	-6	0	-6	-12	-12	0	-15	-9	-6	9
	2	6	0	-18	0	-6	-3	-6	0	-9	-15	3	-3	0	-12
	3	15	12	-3	6	3	12	0	0	-6	0	0	3	9	12
α -PCA	1	-9	-9	0	-9	-9	-6	-9	-18	-6	-3	-3	-9	-9	-3
	2	-3	0	0	0	0	0	0	9	0	0	-27	-6	0	3
	3	3	0	-15	0	-3	-3	-6	12	-6	-18	3	0	0	-12
proPCA	1	-15	-9	3	-9	-6	-9	-6	-9	-3	0	3	-6	-12	0
	2	3	0	0	-3	0	0	-3	0	-3	0	-27	-9	0	3
	3	6	0	-18	0	-6	-3	-6	0	-9	-15	3	-3	0	-12
sPCA	1	-9	-9	0	-9	-9	-6	-9	-18	-6	-3	-3	-9	-9	-3
	2	-3	0	0	0	0	0	0	9	0	0	-27	-6	0	3
	3	3	0	-15	0	-3	-3	-6	12	-6	-18	3	0	0	-12

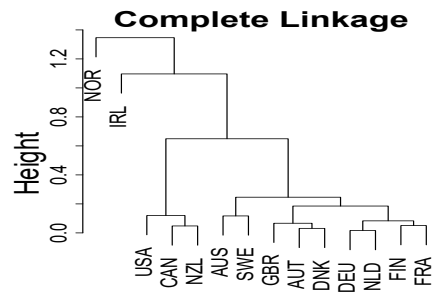
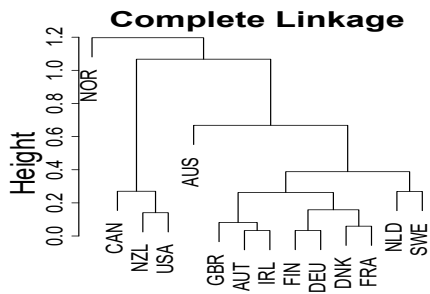
the rotated loadings are multiplied by 30 and then truncated to integers. The estimated loading matrices and corresponding hierarchical clustering results of these methods are shown in Tables 3 and 4, and Figures 9 and 10. For row factors, we can see that the results of the α -PCA and the sPCA are identical, but are different with the autoPCA and the proPCA. For all the methods, the USA, CAN and NZL are clustered into a group. For column factors, it seems that the proPCA has the most similar clustering results with the true index groups, then followed closely by the α -PCA and the sPCA.

Reconstruction comparison in terms of correlation effects: to illustrate the effect of additional row and column information contained in the tensor-decomposition based matrix factor model, we provide the following comparison with the BiMFaM in terms of the signal parts. Denote the estimated signal parts of autoPCA, α -PCA and proPCA as $\hat{\mathbf{S}}_t$, $\tilde{\mathbf{S}}_t$ and $\check{\mathbf{S}}_t$ respectively. We compute the row-wise correlation and column-wise correlation of these methods respectively, and evaluate their performance in terms of the correlation difference heatmap with the true row-wise and the true column-wise correlation of the original data (Figures 1 (a) and (b)). The results are shown in Figures 11 and 12, from where we can see that the pattern of row-wise and column-wise correlation for the TeDFaM is the most similar one to the true correlation. It is also demonstrated by the the distance between the true correlation and the four methods in terms of Frobenius norm, which are 4.3952, 4.4922, 4.4169 and 1.5751 row-wisely, and 3.2226, 3.1133, 2.8567 and 0.8015 column-wisely.

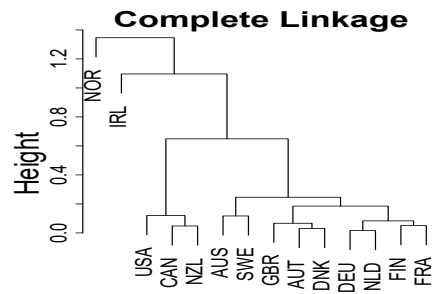
In addition, we also compute the vectorized correlation, and the distance between



(a) hierarchical clustering for autoPCA.

(b) hierarchical clustering for α -PCA.

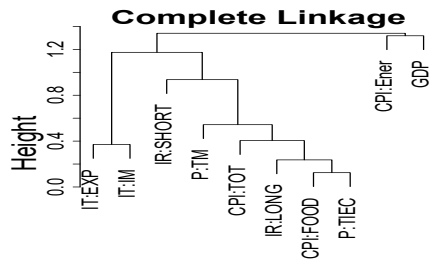
(c) hierarchical clustering for proPCA.



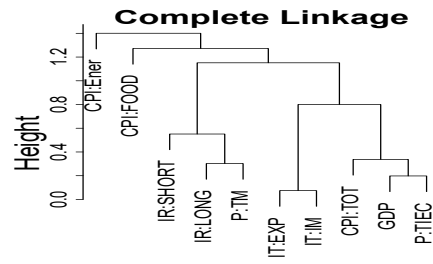
(d) hierarchical clustering for sPCA.

Fig. 9. The hierarchical clustering results for the row loading matrix.**Table 4.** The estimation of the column factor loading matrix C.

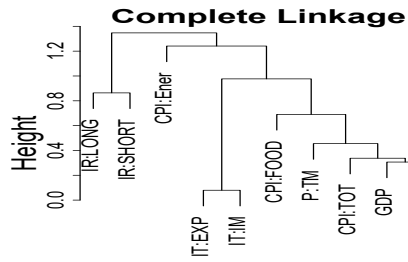
Method	Factor	CPI:Ener	CPI:FOOD	CPI:TOT	GDP	IR:LONG	IR:SHORT	IT:EXP	IT:IM	P:TIEC	P:TM
autoPCA	1	0	0	0	0	-6	-3	-21	-21	0	3
	2	30	0	9	0	0	0	0	0	0	3
	3	0	0	0	12	3	24	0	-3	3	15
	4	0	3	3	-24	3	12	-6	3	0	0
α -PCA	1	0	0	0	6	3	0	21	21	0	0
	2	30	3	9	3	-3	0	0	0	0	0
	3	0	0	0	3	9	24	0	0	3	12
	4	-3	27	6	3	-6	0	0	0	0	3
proPCA	1	0	3	0	6	3	0	21	21	0	0
	2	27	0	9	3	0	0	0	0	0	0
	3	-3	9	0	6	6	24	0	0	0	12
	4	-3	21	3	6	-21	-6	0	0	0	3
sPCA	1	0	0	0	6	3	0	21	21	0	0
	2	30	3	9	3	-3	0	0	0	0	0
	3	0	0	0	3	9	24	0	0	3	12
	4	-3	27	6	3	-6	0	0	0	0	3



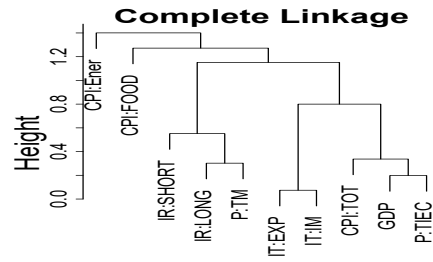
(a) hierarchical clustering for autoPCA.



(b) hierarchical clustering for α -PCA.



(c) hierarchical clustering for proPCA.



(d) hierarchical clustering for sPCA.

Fig. 10. The hierarchical clustering results for the column loading matrix.

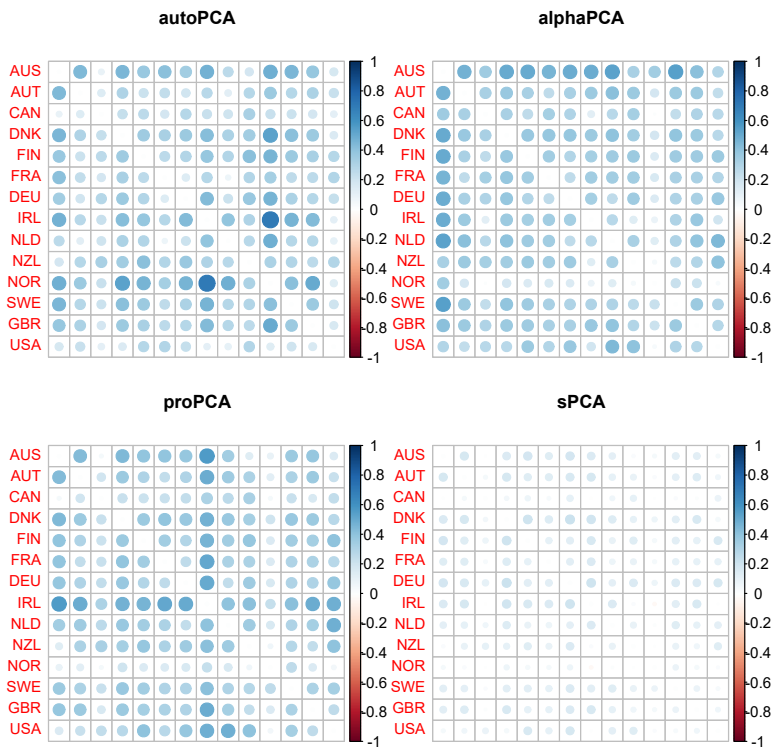


Fig. 11. Comparison of the row-wise correlation

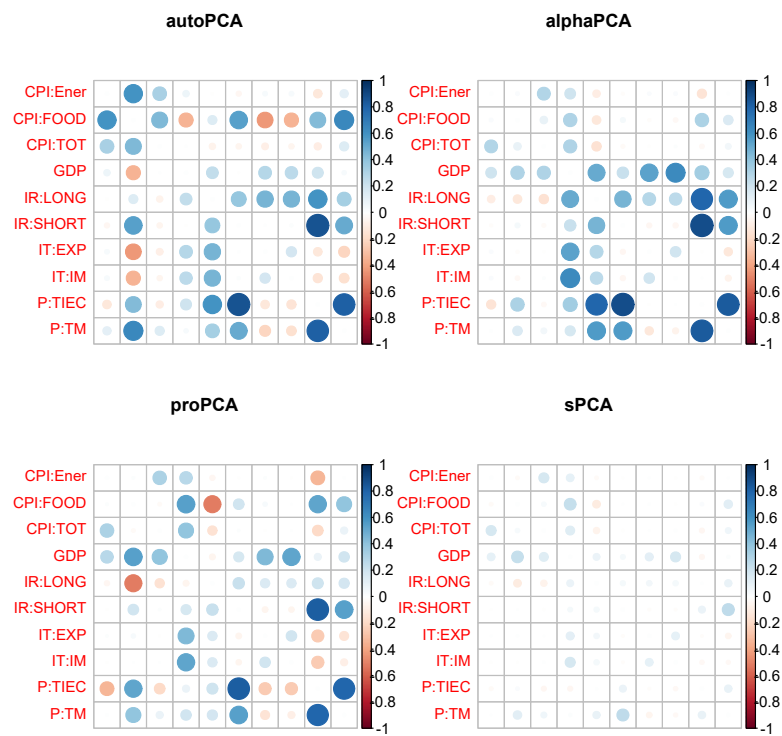


Fig. 12. Comparison of the column-wise correlation

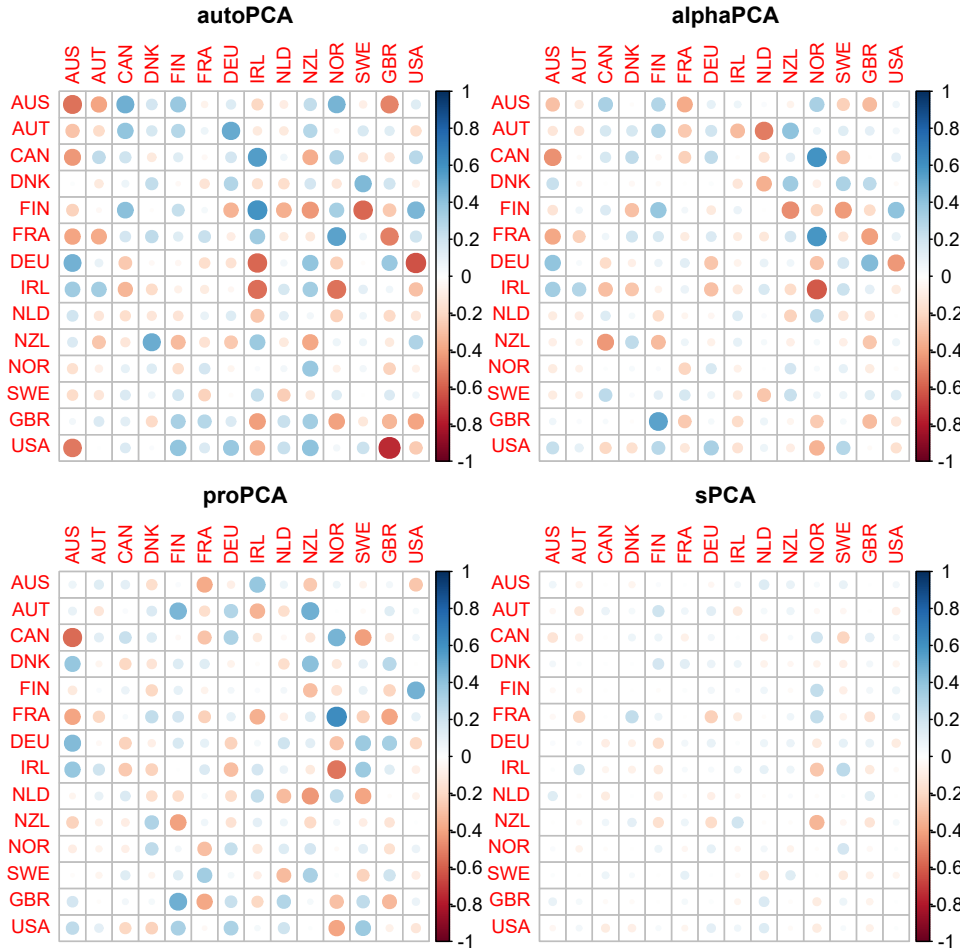


Fig. 13. Comparison of the cross rows and columns correlation

true observations and the four methods are 33.5586, 29.4082, 28.7953 and 11.7576 respectively, and the detailed correlation difference heatmap with Figure 1 (c) is shown in Figure 13, which shows the information extraction sufficiency of the TeDFaM compared to the BiMFaM.

As a result, we explain the reasonability of adding the row and the column parts in the matrix factor model from the view of row, column and vectorization correlation, which demonstrate the reason of better performance in reconstruction, together with Proposition 1.

Reconstruction comparison in terms of RMSE: we use 10 folds cross validation

Table 5. The RMSE values of the four methods for different choice of k_1 and k_2 .

Method	(2, 2)	(3, 4)	(5, 6)	(8, 8)
autoPCA	0.32316	0.27363	0.22717	0.17434
α -PCA	0.30751	0.25963	0.21419	0.15758
proPCA	0.31028	0.26076	0.20676	0.15780
sPCA	0.19788	0.14803	0.08800	0.04290

to evaluate the difference between the observed and estimated matrices. The square root mean squared error (RMSE) is used as measurement at different values of factor numbers. In addition, we also compare with the TCPD method with PCA-type linear combination, whose RMSE is 0.380191. The other results are shown in Table 5, from which we can see that our method performs better than others.

7. Conclusion

To conclude, we identify possible topics for further research. First of all, it is interesting that our technical angle is inverse to that in the preprint (Chang et al., 2021), where they raise the order of the matrix (2nd-order) series to a 3rd-order tensor and model it with the CP decomposition (Kolda and Bader, 2009) with a diagonal core matrix approximation replaced in the bilinear form. Comparatively we apply CP decomposition, which is designed for higher-order tensor factorization, to factorize a matrix that is essentially the low-order tensor, to derive our new matrix factor model with stronger signal. One may conjecture that, under TeDFaM, the estimation accuracy may be further enhanced if the latent factor matrix may be modified properly. Next, the extracted latent factor scores can be regarded as a low-dimensional feature extracted from the original high-dimensional tensor observation, and it can be used for some further research aim such as prediction or clustering. Another direction is, the BiMFaM has been extended to the tensor observations in time series field (Chen et al., 2022), then how to extend TeDFaM to tensor case is an interesting working direction. Finally, the current modelling ignores the extra information for some modes, such as the macronomic index, the demographic characteristics of the countries. Whether incorporate these information into the model

can improve its performance is also left for further studies (Chen et al., 2020b).

References

- Athreya, K. B. and Lahiri, S. N. (2006) *Measure Theory and Probability Theory*, vol. 19. Springer.
- Bai, J. (2003) Inferential theory for factor models of large dimensions. *Econometrica*, **71**, 135–171.
- Bai, J. and Li, K. (2012) Statistical analysis of factor models of high dimension. *The Annals of Statistics*, **40**, 436–465.
- Ben-Israel, A. and Greville, T. N. (2003) *Generalized Inverses: Theory and Applications*, vol. 15. Springer Science and Business Media.
- Chang, J., He, J., Yang, L. and Yao, Q. (2021) Modelling matrix time series via a tensor CP-decomposition. *arXiv preprint arXiv:2112.15423*.
- Chen, E. Y. and Fan, J. (2021) Statistical inference for high-dimensional matrix-variate factor models. *Journal of the American Statistical Association*, 1–18.
- Chen, E. Y., Tsay, R. S. and Chen, R. (2020a) Constrained factor models for high-dimensional matrix-variate time series. *Journal of the American Statistical Association*, **115**, 775–793.
- Chen, E. Y., Xia, D., Cai, C. and Fan, J. (2020b) Semiparametric tensor factor analysis by iteratively projected SVD. *arXiv preprint arXiv:2007.02404*.
- Chen, R., Yang, D. and Zhang, C.-H. (2022) Factor models for high-dimensional tensor time series. *Journal of the American Statistical Association*, **117**, 94–116.
- Chen, Z., Fan, J. and Wang, D. (2020c) High-dimensional factor model and its applications to statistical machine learning. *Scientia Sinica Mathematica*, **50**, 447–490.
- Dawid, A. P. (1981) Some matrix-variate distribution theory: notational considerations and a bayesian application. *Biometrika*, **68**, 265–274.

- Ding, S. and Dennis Cook, R. (2018) Matrix variate regressions and envelope models. *Journal of the Royal Statistical Society: Series B (Statistical Methodology)*, **80**, 387–408.
- Fan, J., Li, R., Zhang, C.-H. and Zou, H. (2020) *Statistical Foundations of Data Science*. Chapman and Hall/CRC.
- Fan, J., Liao, Y. and Mincheva, M. (2013) Large covariance estimation by thresholding principal orthogonal complements. *Journal of the Royal Statistical Society: Series B (Statistical Methodology)*, **75**, 603–680.
- Fan, J., Ma, C. and Zhong, Y. (2021) A selective overview of deep learning. *Statistical Science: A Review Journal of the Institute of Mathematical Statistics*, **36**, 264.
- Francq, C. and Zakoian, J.-M. (2019) *GARCH Models: Structure, Statistical Inference and Financial Applications*. John Wiley and Sons.
- Guo, X., Liu, X., Zhu, E. and Yin, J. (2017) Deep clustering with convolutional autoencoders. In *International Conference on Neural Information Processing*, 373–382. Springer.
- Gupta, A. K. and Nagar, D. K. (2018) *Matrix Variate Distributions*, vol. 104. CRC Press.
- Hinton, G. E. and Salakhutdinov, R. R. (2006) Reducing the dimensionality of data with neural networks. *Science*, **313**, 504–507.
- Hoff, P. D. (2011) Separable covariance arrays via the Tucker product, with applications to multivariate relational data. *Bayesian Analysis*, **6**, 179–196.
- Kolda, Tamara, G. and Bader, Brett, W. (2009) Tensor decompositions and applications. *SIAM Review*, **51**, 455–500.
- Lam, C. and Yao, Q. (2011) Estimation of latent factors for high-dimensional time series. *Biometrika*, **98**, 901–918.
- (2012) Factor modeling for high-dimensional time series: inference for the number of factors. *The Annals of Statistics*, 694–726.

- Li, B., Kim, M. K. and Altman, N. (2010) On dimension folding of matrix-or array-valued statistical objects. *The Annals of Statistics*, **38**, 1094–1121.
- Lu, H., Plataniotis, K. N. and Venetsanopoulos, A. (2013) *Multilinear Subspace Learning: Dimensionality Reduction of Multidimensional Data*. CRC Press.
- Merris, R. (1997) *Multilinear Algebra*. CRC Press.
- Salomon, D. (2004) *Data Compression: the Complete Reference*. Springer Science and Business Media.
- Stock, J. H. and Watson, M. W. (2002) Forecasting using principal components from a large number of predictors. *Journal of the American Statistical Association*, **97**, 1167–1179.
- Suetens, P. (2017) *Fundamentals of Medical Imaging*. Cambridge University Press.
- Wang, D., Liu, X. and Chen, R. (2019) Factor models for matrix-valued high-dimensional time series. *Journal of Econometrics*, **208**, 231–248.
- Yang, X., He, X., Zhao, J., Zhang, Y., Zhang, S. and Xie, P. (2020) COVID-CT-dataset: a CT image dataset about COVID-19. *arXiv preprint arXiv:2003.13865*.
- Ye, J. (2005) Generalized low rank approximations of matrices. *Machine Learning*, **61**, 167–191.
- Yu, L., He, Y., Kong, X. and Zhang, X. (2022) Projected estimation for large-dimensional matrix factor models. *Journal of Econometrics*, **229**, 201–217.
- Zhang, X. (2017) *Matrix Analysis and Applications*. Cambridge University Press.